2011

New Ferrocene Based Dithiolate Ligands

Bahareh Khalili Najafabadi

New Ferrocene Based Dithiolate Ligands

(Thesis format: Monograph)

by

Bahareh Khalili Najafabadi

Graduate Program in Chemistry

A thesis submitted in partial fulfillment
of the requirements for the degree of
Master of Science

The School of Graduate and Postdoctoral Studies
The University of Western Ontario
London, Ontario, Canada

THE UNIVERSITY OF WESTERN ONTARIO
SCHOOL OF GRADUATE AND POSTDOCTORAL STUDIES

CERTIFICATE OF EXAMINATION

Supervisor	Examiners
Dr. John F. Corrigan	Dr. Richard J. Puddephatt
	Dr. Yining Huang
	Dr. Mahi R. Singh

The thesis by

Bahareh Khalili Najafabadi

entitled:

New Ferrocene Based Dithiolate Ligands

is accepted in partial fulfillment of the
requirements for the degree of
Master of Science

Date_____ _____

Chair of the Thesis Examination Board

Abstract

The preparation and characterization of four new ferrocene based dithiolate ligands, which have different spacer groups between the ferrocenyl moiety and the chalcogen centers, are presented. Furthermore, the complexation of ferrocene based dithiolate ligands to platinum, using the oxidative addition of the S-S bonds to Pt(0), is described. Moreover, the preparation of silylated reagents from the synthesized ligands and their use in cluster assembly are studied.

Cyclic voltammetry and UV-Vis absorption spectroscopy experiments were conducted on the synthesized ligands, complexes and cluster, and their results are presented here.

Keywords:

Ferrocene, ferrocenyl, dithiolane, dithiolate, chalcogen, chalcogenolate, nanocluster, silylated reagent, cyclic voltammetry, X-ray crystallography.

Acknowledgements

It is my pleasure to thank those who have made this thesis possible. First and foremost, I offer my greatest gratitude to my supervisor, Dr. John F. Corrigan, who has supported me throughout my study with his patience and knowledge, whilst allowing me to work in my own way. He provided me with constant encouragement and invaluable resources in various ways. I am indebted to him more than he knows. I would like to thank John also for solving and refining the structure of my $C_{18}H_{24}FeNOS_2$ ligand.

I am also thankful to the chemistry staff for the effort and support they offered. People in the NMR, mass spectrometry and X-ray facilities are thanked for their assistance during characterization of all of my compounds.

I am grateful to my colleagues for supporting me, and for truly being the best labmates ever! I would like to express my gratitude, especially to Dr. Dan MacDonald and Chhatra Khadka who kindly guide me through the basic steps of working in the lab. I should also thank my other labmates, Taylor Battista, Tetyana Levchenko, Brian Nikkel and Mahmoud Fard.

I wish to thank my great friends back in Iran and here in Canada for all the friendship and caring they always had for me. I would also like to thank my best friend and love, Amin Torabi, for his kindness, love and encouragement.

Finally, I would like to extend my greatest thanks and appreciation to my family for all of their unconditional love and support, while I am away from them. My love for them is eternal.

TABLE OF CONTENTS

LIST OF FIGURES

LIST OF SCHEMES

LIST OF TABLES

LIST OF ABBREVIATIONS

Å.....angstrom

br.....broad

^{n}Bu.....*n*-butyl

^{t}Bu.....*tert*-butyl

CB.....conduction band

Cp.....cyclopentadienyl

CV.....cyclic voltammetry

DMF.....dimethylformamide

E.....chalcogen atom

EDX.....energy dispersive X-ray

Fc.....CpFe(η^5-C_5H_4)

g.....gram

HRMS.....high resolution mass spectrometry

HSQC.....heteronuclear single quantum correlation

IR.....infra red

M.....any metal atom

Me.....methyl

MHz.....megahertz

ml.....millliter

mmol.....millimol

nm.....nanometer

NMR.....nuclear magnetic resonance

OAc.....acetate anion

Ph.....phenyl

^{n}Pr.....*n*-propyl

R.....organic side group

s (NMR)...singlet

SCE.....saturated calomel electrode

THF.....tetrahydrofuran

UV-Vis...ultraviolet–visible

VB.....valence band

1 Introduction

1.1 Metal Chalcogenide Cluster Chemistry

Metal chalcogenide cluster chemistry is an interesting area of research, and has had great developments in the past several years. The size-dependent chemical, physical and structural properties observed for these materials compared to those of the corresponding bulk materials attracts the attention of researchers from all areas of science.[1, 2] This class of clusters and nanoparticles, contains metal atoms bridged by chalcogens (S, Se, Te). These clusters and nanoparticles exist with and without (surface) shielding ligands.[3] Chalcogenide ions E^{2-} (E = S, Se or Te) successfully bridge most metals and in the most cases are stable to hydrolysis. The high negative charge in combination with large polarizability of these ions causes this tendency for bridging. HE^-, RE^- and E_x^{2-} are other chalcogenide ligands that are known to bridge. The neutral ligands in this family such as E_x, R_2E, and REH are weaker ligands that form much weaker bridging interactions between metals. Since chalcogenide ligands E^{2-} are relatively uncommon as terminally bonded ligands, the preparation of metal chalcogen clusters requires the use of surface capping ligands such as tertiary phosphines, amines, or organochalcogenolate anions (RE^-) to kinetically stabilize a cluster core, thus preventing condensation to the corresponding bulk solid.[4, 5]

The scale of polynuclear metal chalcogenides ranges from small molecules with three metal atoms to colloids of micron dimensions.[4] Although the terms 'cluster' (or nanocluster) and 'nanoparticle' are often used interchangeably in the literature, for the purposes of this thesis the former will be reserved to describe species that are defined

exactly in chemical composition and structure (typically via single X-ray analysis) whereas the term 'nanoparticle' will be reserved for particles with less defined composition, often linked with a certain size distribution.[3]

1.2 Semiconductor Nanomaterials and the Quantum Confinement Effect

In the world of nanotechnology, the term 'nano' describes materials with at least one dimension in the range of 1-100 nm. There are different subclasses for these materials such as thin films, nanoparticles, quantum dots, nanowires and nanoclusters, which show different physical and chemical properties.[6, 7] Numerous research groups are interested in the area of semiconductor nanomaterials because of the unique size-dependent optical and electronic properties observed in the transition from bulk semiconductor material to molecular solid.[1]

Fig. 1.1 presents a schematic energy diagram of the electronic structure of bulk semiconductors (left), nanoparticles (center), and molecules (right).[1] The lower energy region is called valence band (VB) and is usually filled in bulk metals and semiconductors. The upper region is named the conduction band (CB) and is typically unoccupied.[8] When an electron transfers from VB to CB leaves a hole in the conduction band. The so-called quantum confinement effects are observed when the size of the particle becomes on the order of electron-hole pair (exciton). To fit into such a nanometer sized piece of the semiconductor material in question, the exciton must adopt a state of higher kinetic energy. This results an increase in the size of the band gap relative to the bulk solid and the quantization of energy levels within the bands with

decreasing size. For a nanoparticle, the uncertainty in the position of the exciton depends upon its size. The kinetic energy of an exciton in a particle can be derived by employing the parabolic band model: $E_R = E_g + \frac{\eta^2\pi^2}{2R^2}\left[\frac{1}{m_e} + \frac{1}{m_h}\right]$ where E_R is the band gap energy of the nanoparticle, E_g is the band gap energy of the bulk semiconductor, R is the radius of the particle and m_e and m_h are the effective masses of the electron and hole, respectively. Therefore nanoclusters possess electronic properties, which lie between the properties of molecular species and related solids.[6]

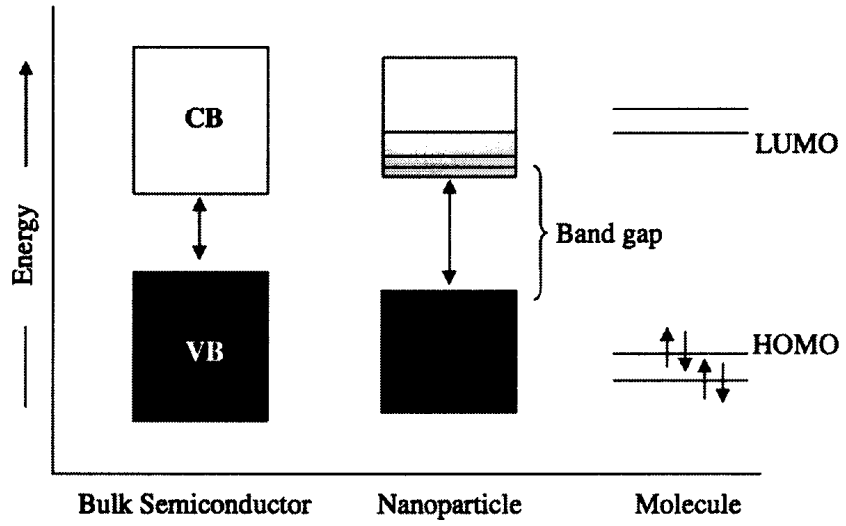

Fig. 1.1 Schematic representation of the electronic structure of bulk semiconductors, nanoparticles, and molecules.[1]

One of the important features of nanometer sized particles and clusters is that the surface-to-volume ratio is much greater than that of the bulk semiconductor, such that the nature of the surface has significant influence on the physical properties.[9] In this respect it has been found that the incorporation of specific ligands onto the surface of nanoclusters can have noticeable effects on the optical and electronic properties of these materials.[5]

1.3 Synthesis of Metal Chalcogenide Clusters, Nanoclusters and Nanoparticles

There are two methodologies for the preparation of metal chalcogenide clusters: top down and bottom up. The top down procedure typically involves the engineering of larger materials into smaller architectures using lithographic, or chemical deposition techniques. The bottom up strategy uses single atoms or ions to grow clusters and nanoparticles.[3] Herein some classes of synthetic reactions are presented.[4]

1.Association of Ions

This is a simple assembly of metal cations and chalcogenide anions, which is practical in the presence of stabilizing ligands.(M=metal, L=ligand, E=S, Se or Te, X = halide, OAc, alkyl, etc.)

$$M^{n+} + E^{2-} \text{ (or } HE^{-} \text{ or } H_2E) + L \rightarrow [M_xE_yL_w]^z \qquad (1.1)$$

2.Direct Reaction of the Elements

Clusters without heteroligands can be synthesized using this method under high temperature conditions. Under milder reaction conditions the presence of ligand is necessary.

$$M + E \rightarrow [M_xE_y] \qquad (1.2)$$

$$M + E + L \rightarrow [M_xE_yL_w] \qquad (1.3)$$

3.Reduction of Chalcogen with Metal Chalcogenolate

This method needs excess chalcogenolate ligand as the terminal ligand.

$$M(E'R)_n + E \rightarrow [M_xE_y(E'R)_w] + RE'E'R \quad (1.4)$$

4.Elimination of Me_3SiX

Elimination of R_3SiX in the reaction of $(R_3Si)_2E$ with a metal salt forms a metal chalcogenide cluster.

$$MX_n + (R_3Si)_2E + L \rightarrow [M_xE_yL_w] + R_3SiX \quad (1.5)$$

5.Reaction of an Anionic Metal Chalcogenide Complex with a Metal Electrophile

Rigid small charged complexes and clusters can react with each other to form larger clusters.

$$[ME_m]^{z-} + [L_nM']^{z+} \rightarrow [(M/M')_xE_yL_w] \quad (1.6)$$

1.4 Silylated Chalcogen Reagents

A powerful method for chalcogen delivery in the synthesis of nanometer-sized metal–chalcogen clusters is the usage of silylated chalcogen reagents.[10] Their utility lies in the fact that they are soluble and easily handled sources of chalcogen which react with metal source under very mild reaction conditions.[11] Silylated reagents ($E(SiMe_3)_2$ or

$E(R)SiMe_3$) react easily with a broad range of metal salts or metal alkyls.[5] Nanoscopic metal-chalcogende clusters have been produced using these reagents.[12, 13] The reactions are driven by the favourable formation of an X-Si bond and the subsequent elimination of by-product $X\text{-}SiMe_3$ (X = halide, OAc, alkyl, etc.). The silane by-product is soluble and usually does not interfere with the crystallization of the formed nanoclusters.[11]

$$M\text{-}X_n + n\ RESiMe_3 \rightarrow [M(ER)_n]_m + n\ X\text{-}SiMe_3 \quad (1.7)$$

$$M\text{-}X_n + n/2\ E(SiMe_3)_2 \rightarrow (ME_{n/2})_2 + n\ X\text{-}SiMe_3 \quad (1.8)$$

$$M\text{-}X_n + n/2\ RESiMe_3 + n/4\ E(SiMe_3)_2 \rightarrow [M(ER)_{n/2}E_{n/4}]_m + n\ X\text{-}SiMe_3 \quad (1.9)$$

In this synthetic procedure, silylated reagents commonly react with the metal salts, themselves typically solubilized by coordinating ligands, at low temperature. The reaction conditions, solvent system, temperature and ancillary ligands can all affect the nuclearity and structure of the product.[2, 11-13] Different sizes of molecular clusters, from small to very large, have been reported utilizing this synthetic method.[5]

There are several approaches to the synthesis of silylated reagents, which are typically straightforward. Preparation of two new silylated reagents is presented in Chapter 3 of this thesis.

1.5 Ferrocene as a functional material

Ferrocene (bis(η^5-cyclopentadienyl)iron(II)) was first discovered in 1951 by Pauson and Kealy[14] and its sandwich structure (Fig. 1.2) was confirmed by X-ray crystallography later in 1956.[15] Since then, this air stable and easily prepared metal

'sandwich' compound has played an important role in the field of organometallic chemistry.[16] Due to its stability and inexpensive commercial availability, ferrocene is more widely used in organometallic chemistry comparing to other metallocenes ($M(C_5H_5)_2$, M = Cr, Co, Ni, Zr, Ti, V, Mo, W, Zn). The stability of ferrocene is due to the covalent bonding arrangement that it shows. The six π electrons of each cyclopentadienyl (Cp) ring and the six *d* electrons of Fe^{2+} are involved in this covalent bonding system. Nine molecular orbitals in this system are filled and therefore ferrocene presents the stability of an 18 electron complex. [17]

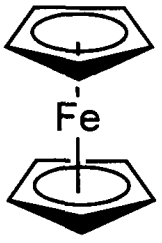

Fig. 1.2 Sandwich structure of ferrocene

The Cp rings in ferrocene can be easily functionalized using reactions characteristic for aromatic compounds. Ferrocene can be selectively mono substituted on one of the Cp rings or di substituted on both rings. ^{t}Butyl lithium in the presence of ^{t}BuOK and ^{n}butyl lithium are used for the preparation of mono- and di-lithioferrocene, respectively. The prepared lithioferrocenes then can be used to generate other functionalized ferrocene compounds. Due to the fact that ferrocene shows greatly adaptable synthetic chemistry, numerous functionalizations have been done on ferrocene and these compounds have had applications in different areas including catalysis, sensing and biology.[16] For example, several successful functionalizations of ferrocene are reported by Beer and coworkers, which have applications in selective sensing of ions

and neutral species (Fig. 1.3).[18] There are also a lot of examples of the functionalization of ferrocene on the surface of dendrimers[19, 20] and nanoparticles[21] that show sensing applications as well (Fig. 1.4). Two factors are responsible for the recognition of anion or neutral analytes by ferrocenyl compounds: the first factor is H-bonding interactions between the functional group (usually amide) on the ferrocene based receptor and the analyte and, second, the electrostatic attraction of the analyte to the cationic form of ferrocene (see below). In the case of dendrimers, the topology of the sensor is also an important feature that can assist in detection.[21]

Ferrocene undergoes a reversible, one-electron oxidation at a low potential (0.475 V vs SCE in CH_2Cl_2 solvent) to form the stable ferrocenium cation. Functionalization of ferrocene with electron withdrawing groups can shift the oxidation potential in the anodic direction (more positive potential), while electron-donating groups alter the position of the oxidation potential in the cathodic direction (more negative potential). In the recognition process using the ferrocene based sensors, only after oxidation of the ferrocene based receptor are the electrostatic interactions 'switched on'. The interaction between receptor and ion, which forms a stable complex, can be detected electrochemically. Cyclic voltammetry experiments usually are used to determine the shifts in the oxidation potentials.[22]

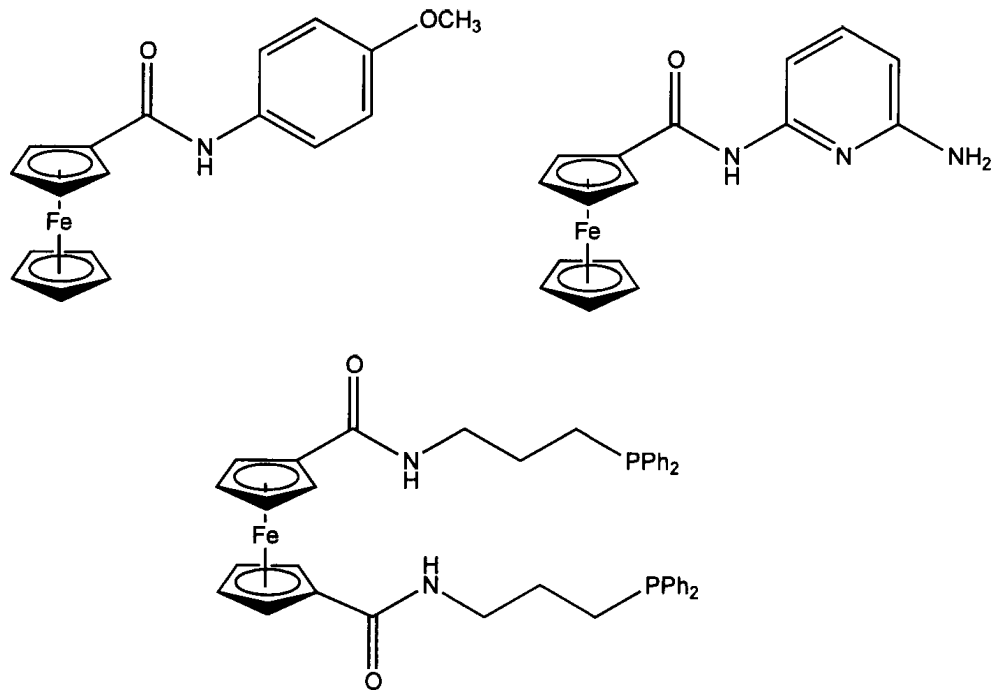

Fig. 1.3 Ferrocene-amide receptors prepared by Beer *et al.*[18]

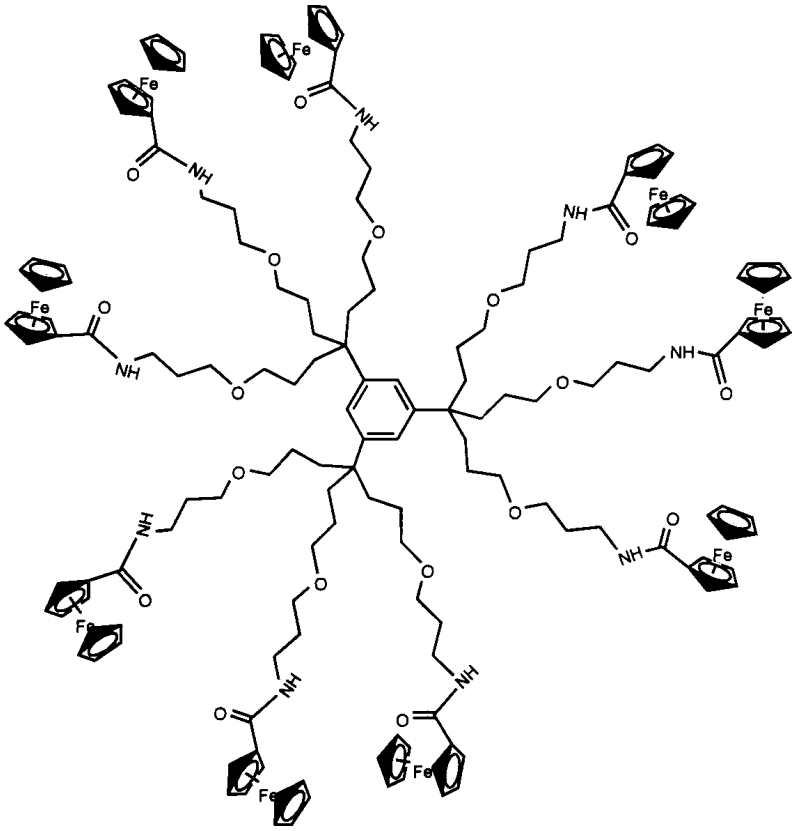

Fig. 1.4 Astruc's ferrocene dendrimer[21]

As mentioned above, the surface-to-volume ratio is much greater for semicondcutor nanoclusters and nanoparticles than that of the bulk semiconductor and the nature of the surface has much more effect on the physical properties of these materials.[9] It has been shown that the incorporation of specific ligands onto the surface of nanoclusters has significant effects on the optical and electronic characteristics of these compounds.[23] Due to greatly adaptable synthetic chemistry that ferrocene shows, its electronic properties, and its accessible ferrocene/ferrocenium redox couple, the ferrocene moiety is a great choice to be incorporated onto the surface of semiconductor nanoclusters.[16] The assembly of ferrocenyl units onto the surface of both small and high-nuclearity clusters opens the door for a wide range of applications, including sensing and molecular electronic devices.[24, 25]

1.6 Project Objectives

Recently, the incorporation of ferrocene based ligands on the surface of metal chalcogenide clusters has been effectively carried out utilizing $CpFe(C_5H_4SeSiMe_3)$ and $Fe(C_5H_4SeSiMe_3)_2$ reagents. It was observed that the oxidation of the ferrocenyl units resulted in oxidative cleavage of the ferrocenylselenolate groups on the cluster surface and cluster degradation.[26, 27] It has been demonstrated that the presence of a spacer between the cluster core and ferrocenyl moieties is helpful in avoiding the oxidative degradation.[21, 25] To this, ferrocenyl based ligands that contained an alkyl chain spacer to limit communication between the ferrocene and chalcogen units such as $FcCH_2SSiMe_3$, $FcC\{O\}OCH_2CH_2ESiMe_3$ (E = S, Se) and $FcC\{O\}NHCH_2CH_2SSiMe_3$ have been used for the assembly of redox stable polynuclear complexes with multiple ferrocenyl units.

These ligands show great utility as powerful precursors for the generation of structurally characterizable metal-chalcogen nanoclusters.[23, 28]

The focus of this research is to target new ferrocene based dithiolate ligands containing an insulating bridge between the ferrocenyl unit and the chalcogen center. Due to the fact that dithiolate ligands have two points of attachment to the cluster core, they may show an increase in the stability of the corresponding nanoclusters in solution compared to monodentate counterparts. An amide functionality may make these ligands effective for oxo-anion recognition. In this thesis the preparation of four ferrocenyl dithiolane compounds is described. Two of these compounds were ligated to the platinum centers to test their reactivity, which formed *cis* mononuclear complexes. The formation of the silylated reagents of dithilane compounds and their reaction with solubilized silver acetate are also discussed. The structure and properties of the synthesized materials are examined using different characterization methods such as X-ray crystallography, NMR and UV-Visible absorption spectroscopy. Cyclic voltammetry studies were also performed to probe the redox activity of the formed compounds.

1.7 References for Chapter 1

(1) Meyer, T. J. In *Comprehensive coordination chemistry II : from biology to nanotechnology;* Jon A. McCleverty, Thomas J. Meyer, Ed.; Elsevier Pergamon: Amsterdam ; Boston, 2004; Vol. 7.

(2) Dehnen, S.; Eichhofer, A.; Fenske, D. Chalcogen-bridged copper clusters. *Eur. J. Inorg. Chem.* **2002**, 279-317.

(3) Schmid, G.; Fenske, D. Metal clusters and nanoparticles INTRODUCTION. *Phil. Trans. R. Soc. A* **2010**, *368*, 1207-1210.

(4) Karlin, K. D., Ed.; In *Progress in inorganic chemistry;* Wiley: New York, 1994; Vol. 41, pp 848.

(5) MacDonald, D. G.; Corrigan, J. F. Metal chalcogenide nanoclusters with 'tailored' surfaces via 'designer' silylated chalcogen reagents. *Phil. Trans. R. Soc. A* **2010**, *368*, 1455-1472.

(6) Rao, C. N. R.; Muller, A.; Cheetham, A. K., Eds.; In *The chemistry of nanomaterials :synthesis, properties and applications;* Wiley-VCH: Weinheim, 2004; Vol. 2, pp 741.

(7) Rao, C. N. R.; Kulkarni, G. U.; Thomas, P. J.; Edwards, P. P. Size-dependent chemistry: Properties of nanocrystals. *Chem. –Eur. J.* **2002**, *8*, 29-35.

(8) Housecroft, C. E.; Sharpe, A. G. In *Inorganic chemistry;* Prentice Hall: Harlow, 2001, pp 808.

(9) DeGroot, M. W.; Taylor, N. J.; Corrigan, J. F. Molecular nanocluster analogues of CdSe/ZnSe and CdTe/ZnTe core/shell nanoparticles. *J. Mater. Chem.* **2004**, *14*, 654-660.

(10) Schmid, G. In *Clusters and colloids :from theory to applications;* VCH: Weinheim; New York, 1994, pp 555.

(11) DeGroot, M. W.; Corrigan, J. F. Metal–Chalcogenolate Complexes with Silyl Functionalities: Synthesis and Reaction Chemistry. *Z. Anorg. Allg. Chem.* **2006**, *632*, 19-29.

(12) Fenske, D.; Ohmer, J.; Hachgenei, J.; Merzweiler, K. New transition metal clusters with ligands from main groups five and six. *Angew. Chem. Int. Ed.* **1988**, *27*, 1277-1296.

(13) Aharoni, A.; Eichhöfer, A.; Fenske, D.; Banin, U. Optical spectroscopy of cadmium-chalcogenide clusters of the type $[Cd_{10}E_4(E'Ph)_{12}(PR_3)_4]$, (E= Te, Se; E'= Se, S). *Opt. Mater.* **2003**, *24*, 43-49.

(14) Kealy, T.; Pauson, P. A new type of organo-iron compound. *Nature* **1951**, *168*, 1039-1040.

(15) Dunitz, J.; Orgel, L.; Rich, A. The crystal structure of ferrocene. *Acta Crystallogr.* **1956**, *9*, 373-375.

(16) Stepnicka, P. In *Ferrocenes :ligands, materials and biomolecules;* J.Wiley: Chichester, England; Hoboken, NJ, 2008, pp 655.

(17) Beswick, M. A.; Palmer, J. S.; Wright, D. S. p-Block metallocenes: the other side of the coin. *Chem. Soc. Rev.* **1998**, *27*, 225-232.

(18) Beer, P. D.; Hayes, E. J. Transition metal and organometallic anion complexation agents. *Coord. Chem. Rev.* **2003**, *240*, 167-189.

(19) Ornelas, C.; Ruiz Aranzaes, J.; Cloutet, E.; Alves, S.; Astruc, D. Click assembly of 1, 2, 3 - triazole - linked dendrimers, including ferrocenyl dendrimers,

which sense both oxo anions and metal cations. *Angew. Chem. Int. Ed.* **2007**, *119*, 890-895.

(20) Astruc, D.; Ornelas, C.; Ruiz Aranzaes, J. Ferrocenyl-terminated dendrimers: Design for applications in molecular electronics, molecular recognition and catalysis. *J. Inorg. Organomet. Polym.* **2008**, *18*, 4-17.

(21) Astruc, D.; Daniel, M. C.; Ruiz, J. Dendrimers and gold nanoparticles as exo-receptors sensing biologically important anions. *Chem. Commun.* **2004**, 2637-2649.

(22) Beer, P. D.; Bayly, S. R. Anion sensing by metal-based receptors. *Anion Sensing* **2005**, 373-378.

(23) MacDonald, D. G. Ph.D. Thesis, University of Western Ontario, 2010.

(24) Mulrooney, R. C.; Singh, N.; Kaur, N.; Callan, J. F. An "off-on" sensor for fluoride using luminescent CdSe/ZnS quantum dots. *Chem. Commun.* **2009**, 686-688.

(25) Labande, A.; Ruiz, J.; Astruc, D. Supramolecular gold nanoparticles for the redox recognition of oxoanions: Syntheses, titrations, stereoelectronic effects, and selectivity. *J. Am. Chem. Soc.* **2002**, *124*, 1782-1789.

(26) Lebold, T. P.; Stringle, D. L. B.; Workentin, M. S.; Corrigan, J. F. Functionalizing the surface of II-VI clusters: redox active centres on the adamantoid complex $[Cd_4Cl_4\{\mu\text{-}(SeC_5H_4)Fe(C_5H_5)\}_6]^{2-}$ *Chem. Commun.* **2003**, 1398-1399.

(27) Wallbank, A. I.; Corrigan, J. F. 1,1 '-Bis(trimethylsilylseleno)ferrocene in cluster synthesis: a redox active surface on a copper-selenide core. *Chem. Commun.* **2001**, 377-378.

(28) Ahmar, S.; MacDonald, D. G.; Vijayaratnam, N.; Battista, T. L.; Workentin, M. S.; Corrigan, J. F. A Nanoscopic 3D Polyferrocenyl Assembly: The Triacontakaihexa(ferrocenylmethylthiolate)[$Ag_{48}(\mu_4\text{-}S)_6(\mu_{2/3}\text{-}SCH_2Fc)_{36}$]. *Angew. Chem. Int. Ed.* **2010**, *49*, 4422-4424.

2 New Ferrocene Based Dithiolanes

2.1 Introduction

The significant surface-to-volume ratio of semiconductor nanoclusters compared to that of bulk materials results in a great influence of the nature of the surface on the properties of these nano-size compounds.[1] In this respect it has been found that the incorporation of specific ligands onto the surface of nanoclusters has noticeable effects on the optical and electronic properties of these materials.[2] Because of the fact that ferrocene shows a greatly adaptable synthetic chemistry, and its accessible ferrocene/ferrocenium redox couple, the ferrocene moiety is a great choice to be incorporated onto the surface of semiconductor nanoclusters for the preparation of polyferrocenyl assemblies.[3]

There are numerous successful strategies for polyferrocenyl assembly including the functionalization of dendrimers[4], polymers[5], the surfaces of metal nanoparticles[6] and supramolecular assemblies[7] with these redox active moieties. Both small and high-nuclearity clusters with ferrocenyl units on their surfaces have potential for a variety of applications such as in sensing and in the preparation of molecular electronic devices.[8, 9]

It has been previously observed for metal chalcogen nanoclusters containing $[CpFe(C_5H_4Se)]^-$ and $[Fe(C_5H_4Se)_2]^{2-}$, that the oxidation of the ferrocenyl units (Fe(II) to Fe(III)) resulted in oxidative cleavage of the ferrocenylselenolate groups and cluster degradation.[10, 11] However it has also been shown that the usage of a spacer between the cluster core and ferrocenyl moieties is successful in preventing that oxidative

degradation.[8, 12] Importantly, the spacer moiety can contain some specific chemical feature such as an amide group, which can ultimately be effective for oxo-anion recognition.[8]

With these aspects in mind we targeted the synthesis of new ferrocene based dithiolate ligands containing an insulating bridge between the ferrocenyl unit and the chalcogen center. Dithiolate ligands may have stronger attachment to the metals and increase the stability of the corresponding nanoclusters in solution. The ligand may ultimately be less likely to detach from the cluster core, thus prevents the aggregation of the clusters in solution. An amide, ester or carbonyl functionality may make these ligands effective for anion recognition studies. These ligands could then be utilized in the development of novel functionalized semiconductor nanoclusters. This chapter presents the preparation and characterization of four new ferrocene based dithiolane ligands, which have different spacer groups between the ferrocenyl moiety and the dithiolane unit. Absorption spectra and cyclic voltammograms of the synthesized ligands also will be described.

2.2 Experimental

2.2.1 General Synthetic Techniques and Starting Materials

All syntheses were performed under a dinitrogen atmosphere using standard Schlenk line and glove box techniques unless otherwise stated. All chemicals were used as received from Strem Chemicals and/or Aldrich. Tetrahydrofuran, diethyl ether, hexanes, and pentane purchased from Caledon were dried by passing through packed columns of activated alumina using a commercially available MBraun MB-SP Series

solvent purification system. Dichloromethane, chloroform and chloroform-d were purchased from Caledon, and distilled over P_2O_5. Ferrocenyl amine, ferrocenyl methanol and 2-(1, 2-dithiolan-3-yl)acetic acid were prepared following literature procedures.[13-15]

^1H and $^{13}C\{^1H\}$ NMR spectra were obtained on a Varian Mercury 400 MHz spectrometer and are reported in ppm. These spectra were referenced internally to solvent peaks relative to $SiMe_4$ at δ=0 ppm.

Single crystal X-ray diffraction measurement was performed on a Bruker APEXII diffractometer, with the molecular structures determined via direct methods using the SHELX suite of crystallographic programs (G.M. Sheldrick, Madison, WI). A BAS 100 electrochemical workstation using a 3-electrode system, with glassy carbon working electrode, platinum flag counter electrode, and a silver wire reference electrode with 0.1 M $[NBu_4][BF_4]$ in CH_2Cl_2 as the supporting electrolyte was used for electrochemical measurements. The potentials are reported versus saturated calomel electrode (SCE) and were referenced internally to ferrocene (475 mV),[16] added at the end of the experiments. Ultraviolet-visible (UV-Vis) absorption spectra were recorded on a Varian Cary 300 Bio UV-Vis spectrophotometer in CH_2Cl_2. Infrared (IR) absorption spectra were obtained on a Bruker Vector 33 IR spectrophotometer in the solid state. A film of solid was formed on the surface of a NaCl crystal cell by evaporating the solvent of a concentrated solution of the compound of interest. High-resolution mass spectra were recorded on a MAT8400 mass spectrometer.

All reactions have been completed in subdued light due to the sensitivity of S-S bonds in these compounds.[17]

2.2.2 *Rac*-5-(1, 2-dithiolan-3-yl)pentanoic acid chloride (1):

Lipoic acid (0.20 g, 0.97 mmol) was dissolved in 10 ml of toluene to which DMF (0.02 ml, 20 mol %) was added as a catalyst. Oxalyl chloride (0.10 ml, 1.16 mmol) in 3 ml of toluene was added dropwise to the solution. It was stirred for 5-10 min (until no further gas was observed) and used directly for subsequent steps.[18-20]

2.2.3 *N*-ferrocenyl-*rac*-5-(1, 2-dithiolan-3-yl)pentanamide (2):

Ferrocenyl amine (0.16 g, 0.77 mmol) was dissolved in 10 ml of dichloromethane. Triethylamine (0.14 ml, 0.97 mmol) was added and the yellow solution was cooled to 0 °C. Freshly prepared lipoic acid chloride (0.97 mmol) in toluene was added. The solution was stirred at 0 °C for 30 min and at room temperature for 20 hours. It was then diluted with 20 ml of dichloromethane and washed with 1M NaOH, saturated NaCl, 1M HCl and NaCl aqueous solutions. The organic layer was separated and dried over $MgSO_4$. The solvent was removed *in vacuo* yielding 0.20 g (66%) of compound **2** as an orange-brown solid.

^{1}H NMR (400 MHz, $CDCl_3$, 5mM, 23°C) δ = 6.47 (br.s, 1H), 4.57 (vt, J_{HH}=2.0 Hz, 2H), 4.14 (s, 5H), 3.98 (vt, J_{HH}=2.0 Hz, 2H), 3.58 (m, 1H), 3.12 (m, 2H), 2.47 (m, 1H), 2.24 (td, $^3J_{HH}$=7.4, $^2J_{HH}$=1.6 Hz, 2H), 1.92 (m, 1H), 1.71 (m, 4H), 1.49 (m, 2H). $^{13}C\{^1H\}$ NMR (100.5 MHz, CDCl3) δ = 170.86 (C(O)), 94.42 (CN), 69.12 (Cp), 64.49 (CH), 61.41 (CH), 56.38 (CHS), 40.23 (CH_2), 38.46 (CH_2S), 36.96 (CH_2), 34.60 (CH_2), 28.82 (CH_2), 25.30 (CH_2). HRMS: Calcd for $C_{18}H_{23}ONS_2Fe$ (*m/z*): 389.0570 Found: 389.0571. Anal. Calc. (%) for $C_{18}H_{23}ONS_2Fe$: C 55.53, H 5.96, N 3.60, S 16.44. Found: C 55.65, H 5.90, N 3.56, S 16.41.

2.2.4 Ferrocenemethyl *rac*-5-(1,2-dithiolane-3-yl)pentanoate (3):

Ferrocenyl methanol (0.17 g, 0.77 mmol) was dissolved in 10 ml of dichloromethane. Triethylamine (0.14 ml, 0.97 mmol) was added and the yellow solution was cooled to 0 °C. Freshly prepared lipoic acid chloride (0.97 mmol) in toluene was added. The solution was stirred at 0 °C for 30 min and at room temperature for 20 hours. It was then diluted with 20 ml of dichloromethane and washed with 1M NaOH, saturated NaCl, 1M HCl and NaCl aqueous solutions. The organic layer was separated and dried over $MgSO_4$. The solvent was removed *in vacuo* yielding 0.27 g (86%) of compound **3** as an air stable orange oil.

^{1}H NMR (400 MHz, $CDCl_3$, 23°C) δ = 4.87 (s, 2H), 4.24 (vt, J_{HH}=1.8 Hz, 2H), 4.15 (vt, J_{HH}=1.8 Hz, 2H), 4.13 (s, 5H), 3.51 (m, 1H), 3.10 (m, 2H), 2.41 (m, 1H), 2.27 (t, $^3J_{HH}$=7.2 Hz, 2H), 1.86 (m, 1H), 1.64 (m, 4H), 1.41 (m, 2H). $^{13}C\{^1H\}$ NMR (100.5 MHz, CDCl3) δ = 172.79 (C(O)), 80.82 (CH_2), 69.12 (CH), 68.36 (CH), 68.10 (Cp), 62.29 (C) 55.84 (CHS), 39.72 (CH_2), 38.03 (CH_2S), 34.09 (CH_2), 33.57 (CH_2), 28.22 (CH_2), 24.21 (CH_2). HRMS: Calcd for $C_{19}H_{24}O_2S_2Fe$ (*m/z*): 404.0567 Found: 404.0562. Anal. Calc. (%) for $C_{19}H_{24}O_2S_2Fe$: C 56.38, H 5.94, S 15.83. Found: C 55.83, H 5.97, S 16.30.

2.2.5 1-ferrocenyl-*rac*-5-(1, 2-dithiolan-3yl)pentan-1-one (4):

Freshly prepared lipoic acid chloride (0.97 mmol) in toluene was added to a solution of ferrocene (0.14 gr, 0.75 mmol) and $AlCl_3$ (0.15 g, 1.12 mmol) in 15 ml of CH_2Cl_2 at 0 °C. The solution was stirred at 0 °C for 15 min and at room temperature for 20 hours. The solution was washed with saturated NaCl aqueous solution (3×20 ml) and

the solvent was removed *in vacuo* to obtain a brown-orange solid. The solid was purified over a silica gel column with 1:3 ethylacetate/ hexane solvent. Yield=17%.

^{1}H NMR (400 MHz, $CDCl_3$, 23°C) δ = 4.76 (vt, J_{HH}=2.0 Hz, 2H), 4.48 (br.s, 2H), 4.18 (s, 5H), 3.61-3.52 (m, 1H), 3.10-3.20 (m, 2H), 2.70 (t, $^3J_{HH}$=7.4 Hz, 2H), 2.43-2.52 (m, 1H), 1.85-1.91 (m, 1H), 1.52-1.80 (m, 4H), 1.45-1.52 (m, 2H). HRMS: Calcd for $C_{18}H_{22}OS_2Fe$ (*m/z*): 374.0461 Found: 374.0456.

2.2.6 *N*-ferrocenyl-*rac*-2-(1,2-dithiolane-3yl)ethylamide (5):

Method A: 2-(1, 2-dithiolan-3-yl)acetic acid (0.37 g, 2.25 mmol) was dissolved in 35 ml of CH_2Cl_2 and HOBt (hydroxybenzotriazole) (0.34 g, 2.52 mmol) was added. The solution was cooled to 0 °C and stirred for 10 min. HBTU (O-benzotriazole-N,N,N′,N′-tetramethyl-uronium-hexafluoro-phosphate) (0.85 g, 2.25 mmol) and 6 ml of triethylamine (4.5 mmol) were added to the solution. It was stirred at room temperature for 1 hour and aminoferrocene (0.50 g, 2.5 mmol) was then added. The solution was diluted with 30 ml of CH_2Cl_2 and stirred for 22 hours. That solution was washed with saturated $NaHCO_3$, 10% citric acid, $NaHCO_3$ aqueous solutions and with water. The organic layer was dried with Na_2SO_4 and the solvent was evaporated under vacuum. The product was purified over a silica gel column with 1:3 ethylacetate/hexane solvent. Yield=34%.

Method B: 2-(1, 2-dithiolan-3-yl)acetic acid (0.14 g, 0.85 mmol) was dissolved in 10 ml of toluene to which DMF (0.01 ml, 20 mol %) was added as a catalyst. Oxalyl chloride (0.09 ml, 1.02 mmol) in 3 ml of toluene was added drop wise to the solution. It was stirred for 5-10 min (until no further gas was observed). This solution was added to

a mixture of ferrocenyl amine (0.14 g, 0.68 mmol) and Et_3N (0.12 ml, 0.85 mmol) in 10 ml of CH_2Cl_2 at 0 °C. It was stirred at 0 °C for 10 min and at room temperature for 25 hours. After that the solution was diluted with 15 ml of CH_2Cl_2, washed with 1M NaOH, saturated NaCl, 1M HCl and NaCl aqueous solutions. The organic layer was separated and the solvent was removed under vacuum. The product was purified over a glass plate covered with silica gel in 2 steps, first with 1:4 ethylacetate/hexane solvent and then with 1:2.5 ethylacetate/hexane solvent for a better separation. Yield=65%.

^1H NMR (400 MHz, $CDCl_3$, 23 °C) δ = 6.73 (br s, 1H), 4.69 (br s, 1H), 4.53 (br s, 1H), 4.18 (s, 5H), 4.14 (m, 1H), 4.02 (br s, 2H), 3.18 (m, 2H), 2.59 (m, 2H), 2.55 (m, 1H), 2.00 (m, 1H). HRMS: Calcd for $C_{15}H_{17}S_2FeON$ (*m/z*): 347.01010 Found: 347.01007.

2.3 Results and Discussion

2.3.1 Synthesis

In order to prepare ligands with two chalcogen centers available for the attachment to the metal chalcogen core and by looking at previously reports in this area[9], ferrocenyl based ligands with five-member dithiolane rings were targeted. The syntheses were started with lipoic acid, which is commercially available. Under irradiation of light or heat the five-membered ring in lipoic acid opens and undergoes polymerization reaction.[17] Thus all reactions involving this five-membered dithiolane ring in the starting reagents or products, have been done in dark and high reaction temperatures have been avoided. All four ligands were synthesised by doing a coupling reaction between a ferrocenyl unit and a five-member dithiolane ring moiety as an acid chloride. Lipoic acid

chloride was synthesised using oxalyl chloride and DMF as a catalyst. (Scheme 2.1). It has been shown previously that DMF can act as a catalyst in the synthesis of acid chlorides using oxalyl chloride.[18, 19]

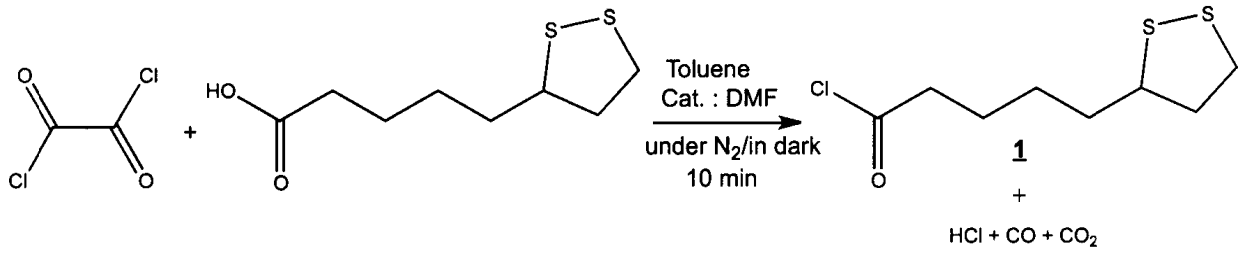

Scheme 2.1 Synthesis of lipoic acid chloride

Compound **2** was obtained as an air stable orange solid in 66% yield, starting from ferrocenyl amine and lipoic acid chloride (Scheme 2.2) and fully characterized with different methods.

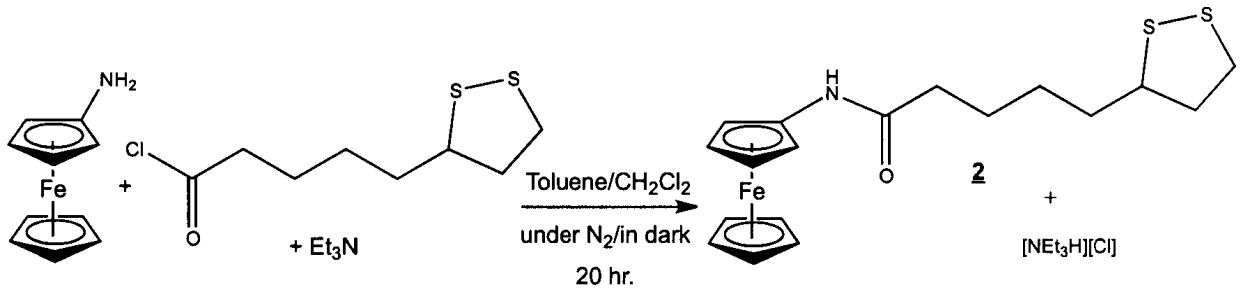

Scheme 2.2 Synthesis of **2** using lipoic acid chloride and ferrocenylamine

Compound **3** was synthesised following a similar procedure using freshly synthesised lipoic acid chloride, ferrocenyl methanol and triethylamine. (Scheme 2.3) The product was obtained as an air stable orange oil in 86% yield.

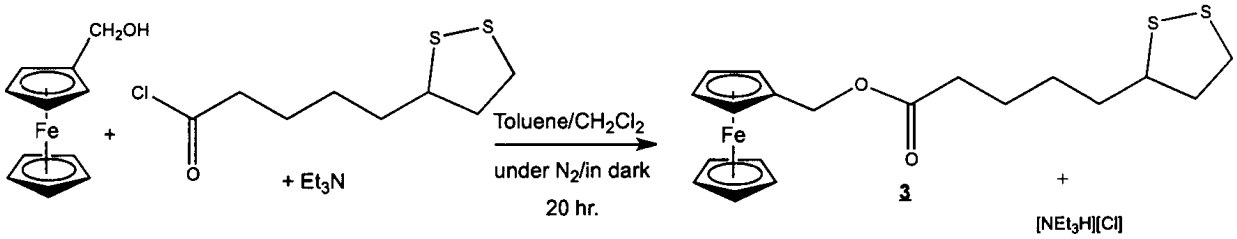

Scheme 2.3 Synthesis of 3 using lipoic acid chloride and ferrocenyl methanol

The Friedel–Crafts acylation of ferrocene to yield 4 was attempted several times with a variety of reaction conditions including different solvents and Lewis acid catalysts ($AlCl_3$, $FeCl_3$, ZnO) but none of them proceeded in sufficient yield for subsequent steps. Due to the thermal sensitivity of the S-S bond in the C_3S_2 ring, this reaction is limited to ambient temperatures, which may be the cause of the low yields. The poor solubility of these catalysts under these conditions (toluene is required for the formation of lipoic acid chloride) is also a likely factor. However compound 4 was synthesised (Scheme 2.4) and characterized via NMR spectroscopy and mass spectrometry.

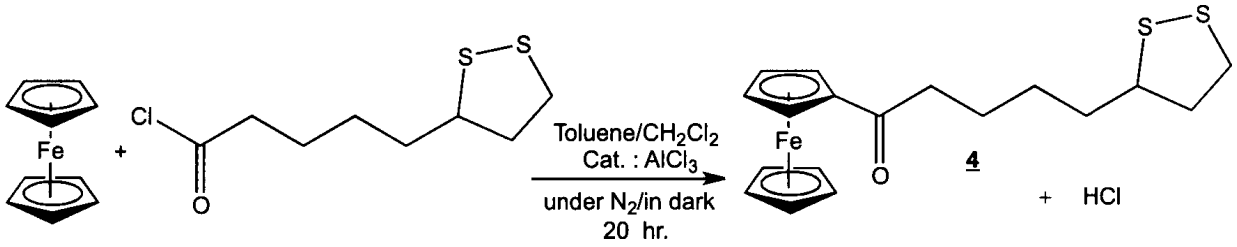

Scheme 2.4 Synthesis of 4 using Friedel-Crafts acylation of ferrocene

For the synthesis of compound 5 the related acid (2-(1, 2-dithiolan-3-yl)acetic acid) was prepared following a literature procedure.[15] Compound 5 can be prepared via two methods, starting from the acid and ferrocenyl amine. In method A, a coupling reaction was done using HOBt/HBTU. In method B (Scheme 2.5), 2-(1, 2-dithiolan-3-

yl)acetic acid was transformed to the related acid chloride and a coupling reaction was done between the acid chloride and ferrocenyl amine. Considering both the purification steps and the final yield for both methods, method B is preferred to prepare compound **5**.

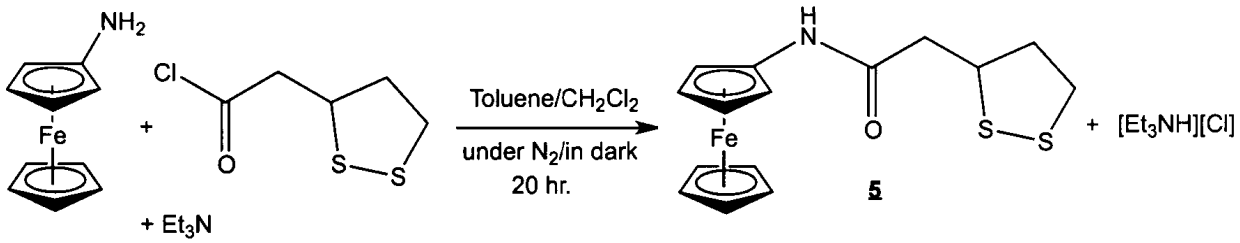

Scheme 2.5 Synthesis of **5** with method B

Although **5** was successfully synthesised and fully characterized, the 5 step procedure for the synthesis of 2-(1, 2-dithiolan-3-yl)acetic acid[15] has a very low yield (15%) and due to the presence of impurities in the product, chromatographic purification is needed. In addition, due to the light sensitivity of both 2-(1, 2-dithiolan-3-yl)acetic acid and **5** it is not found to be practical to prepare **5** in sufficient quantities for subsequent reactions.

2.3.2 Characterization

2.3.2.1 NMR Spectroscopy

All synthesised ferrocenyl based complexes were characterized by NMR spectroscopy and chemical shift data were obtained at room temperature in $CDCl_3$. Due to the complex aliphatic region in their ^1H NMR spectra, 2D NMR spectroscopic methods were used for the assignment of the signals. All peaks in the ^1H NMR spectra were assigned completely using gcosy and gHSQC techniques.

The proton NMR spectrum of compound **2** (Fig. 2.1) shows a slight downfield shift of the Cp proton peaks versus those of ferrocenyl amine. The amine peak in $FcNH_2$ at 2.60 ppm has disappeared and a signal at 6.47 ppm is readily assigned to the presence of an amide. All the assigned peaks are illustrated in Fig. 2.1.

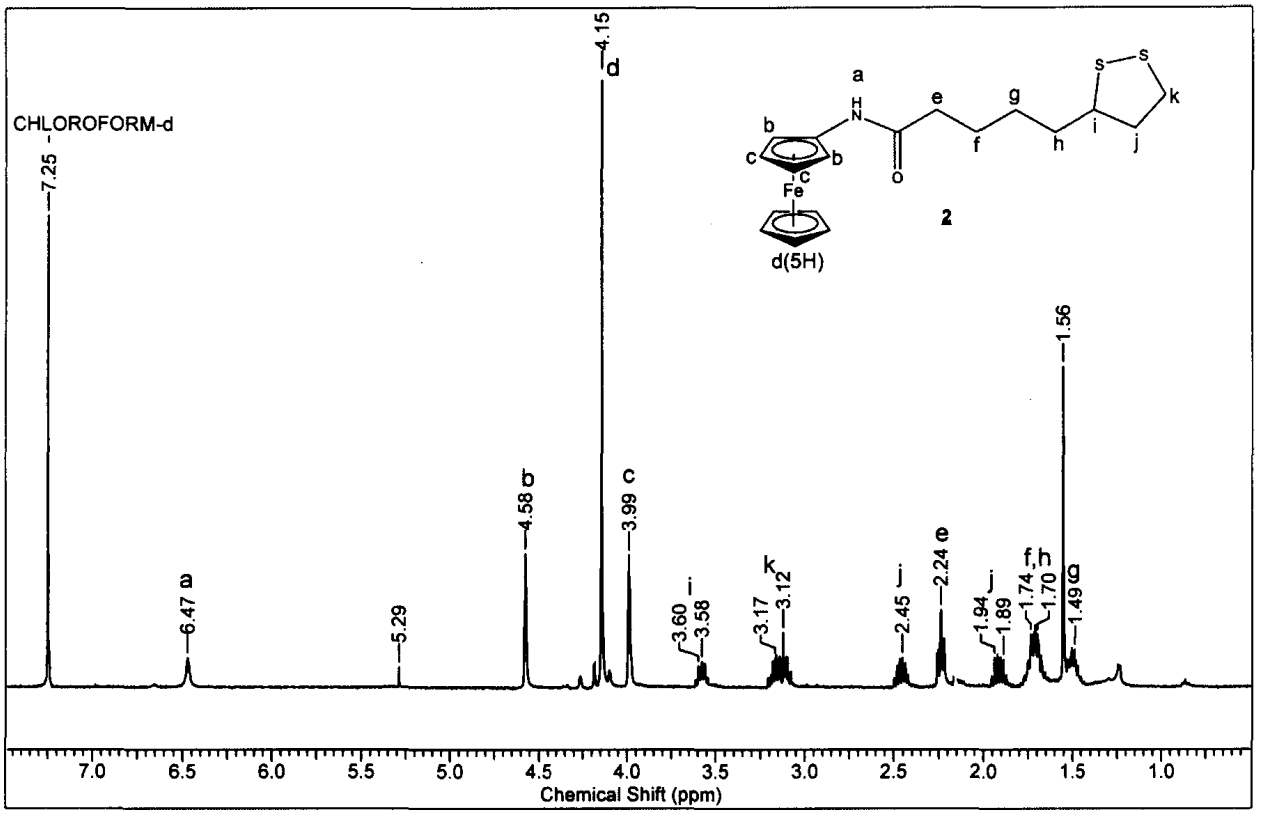

Fig. 2.1 ^1H NMR spectrum of 5 mM of **2** in $CDCl_3$

The proton NMR spectrum of compound **3** displays similar number of peaks in aliphatic region to those reported for **2** with a very slight shift in the chemical shifts due to the replacement of amide group with an ester functional group. The two hydrogen centers in the CH_2 spacer bonded to the cyclopentadienly ring and ester group are assigned to a signal at 4.87 ppm (singlet). The peaks for the hydrogen atoms in the ferrocenyl group are assigned in Fig. 2.2.

In Fig. 2.3 the gcosy NMR spectrum of **3** is illustrated, which was used for the assignment of ^{1}H NMR spectrum of this compound. In this two-dimensional NMR technique the cross-peaks appear between protons that have 3-bond proton-proton scalar coupling ($^3J_{HH}$).

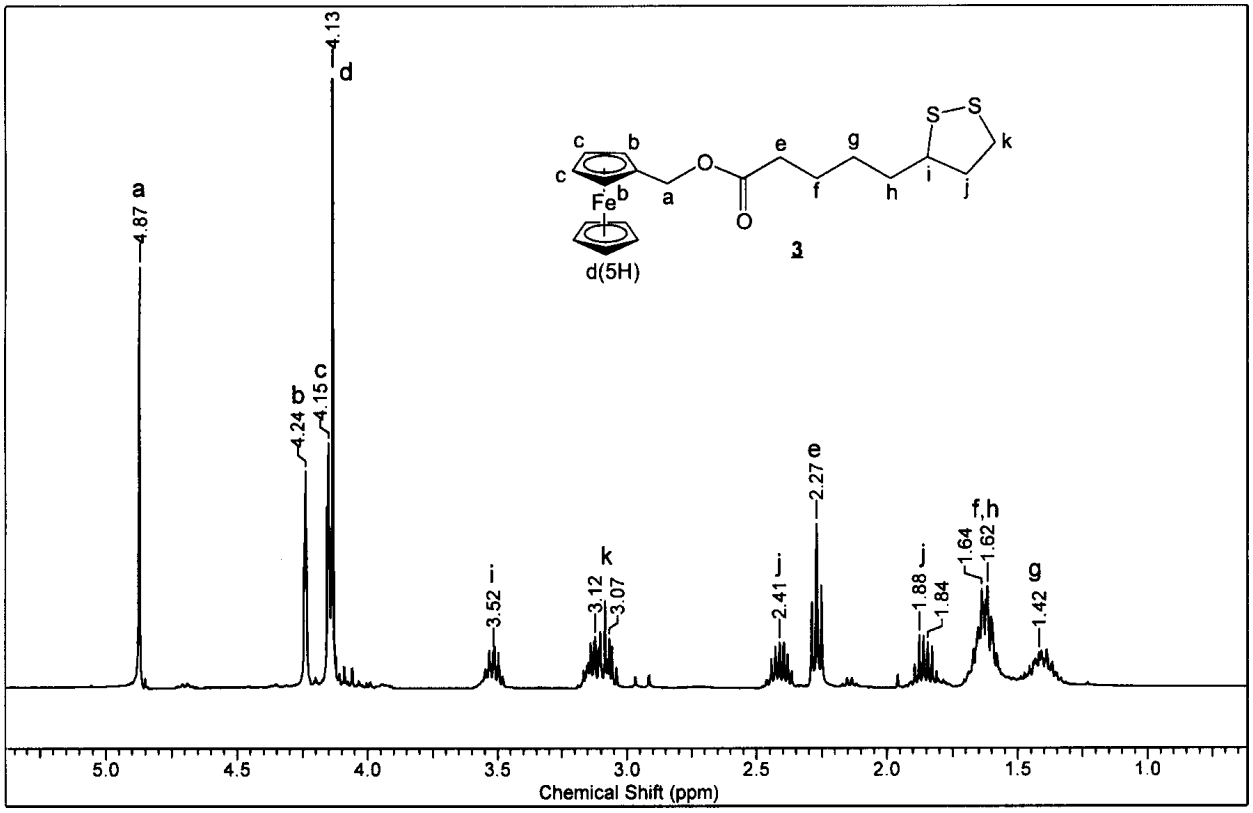

Fig. 2.2 ^{1}H NMR spectrum of **3** in $CDCl_3$

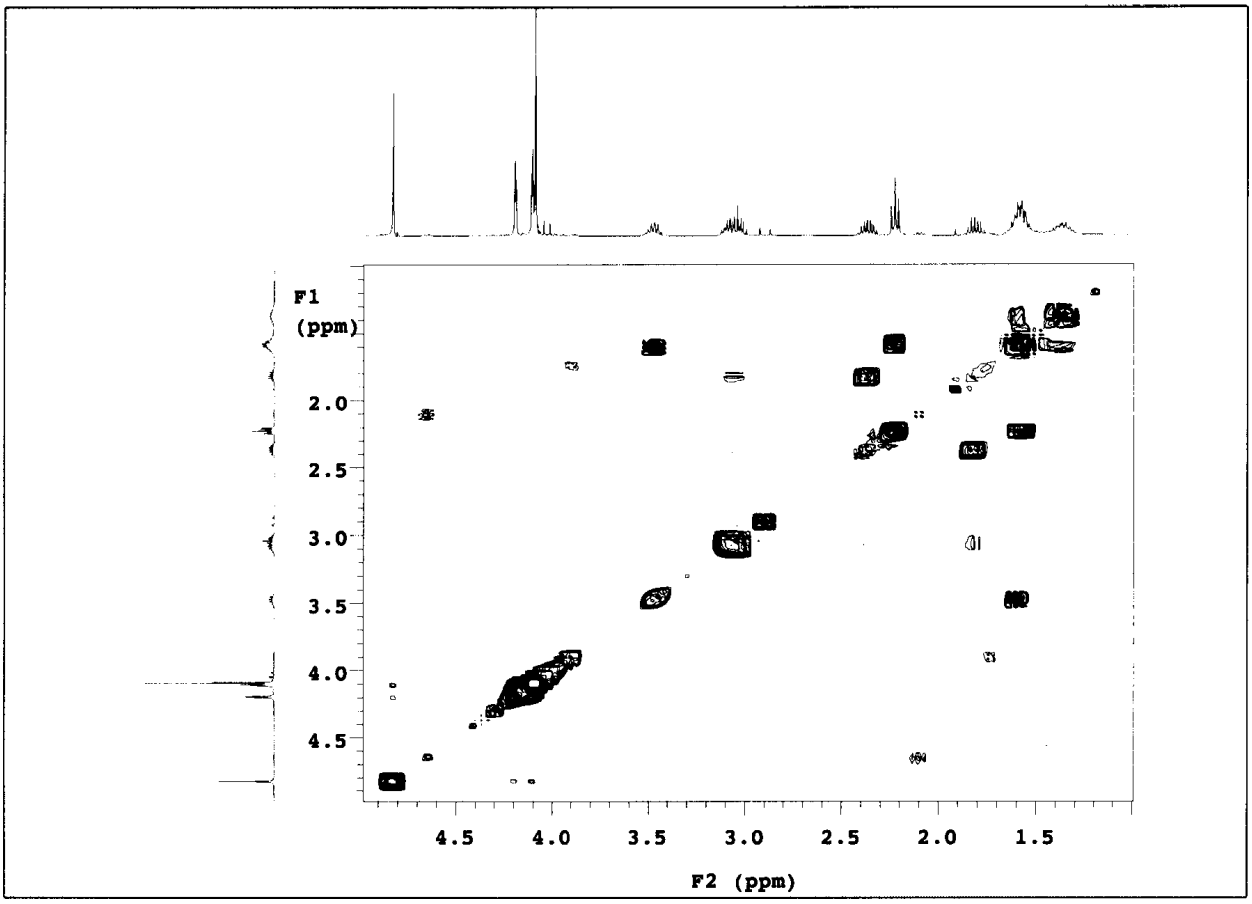

Fig. 2.3 gcosy NMR spectrum of **3** in $CDCl_3$

Similarly the ^1H NMR spectra of **4** and **5** were analyzed using gcosy techniques and via comparison with values reported for similar compounds. The assigned ^1H NMR spectra of **4** and **5** are shown in Fig. 2.4 and Fig. 2.5, respectively.

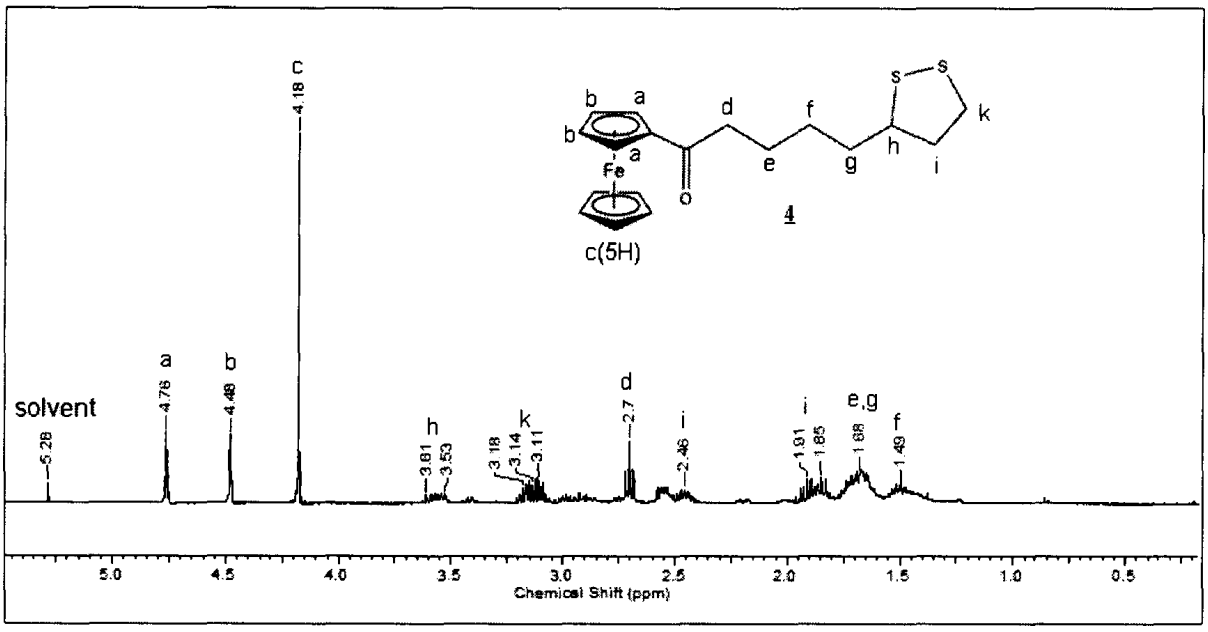

Fig. 2.4 ^{1}H NMR spectrum of 4 in $CDCl_3$

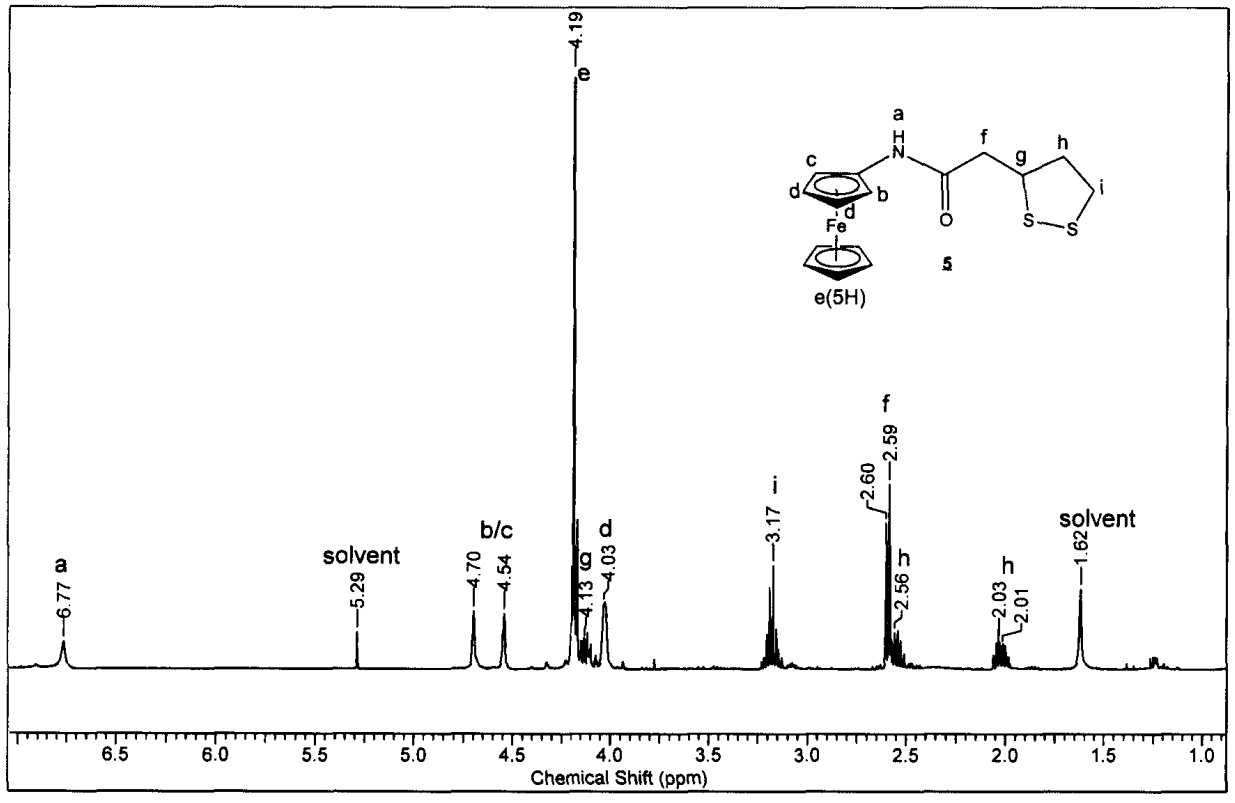

Fig. 2.5 ^{1}H NMR spectrum of 5 in $CDCl_3$

2.3.2.2 UV-Vis Spectroscopy

The absorption spectra of compounds 2, 3 and 5 are presented in Fig. 2.6. They all display a maximum between 440-450 nm with molar absorption coefficients (ε) of 184, 102 and 37 $M^{-1}cm^{-1}$ respectively. These peaks are assigned to the symmetry forbidden d-d transitions in the ferrocenyl moiety of the related compounds, the assignment is based on the UV-Vis absorption spectra of related ferrocenyl amides.[13] Compound 3 shows a well-resolved maximum at 330 nm with ε=255 $M^{-1}cm^{-1}$ which is assigned to the transition from the highest π-orbital to the antibonding σ-orbital in the S-S bond.[21] However, the corresponding peaks in two other spectra are not resolved well and display as shoulders. The position of this shoulder for 2 is also observed ~330 nm with ε = 402 $M^{-1}cm^{-1}$ but for 5 it has a slight shift and is observed ~ 340 nm with ε = 80 $M^{-1}cm^{-1}$.

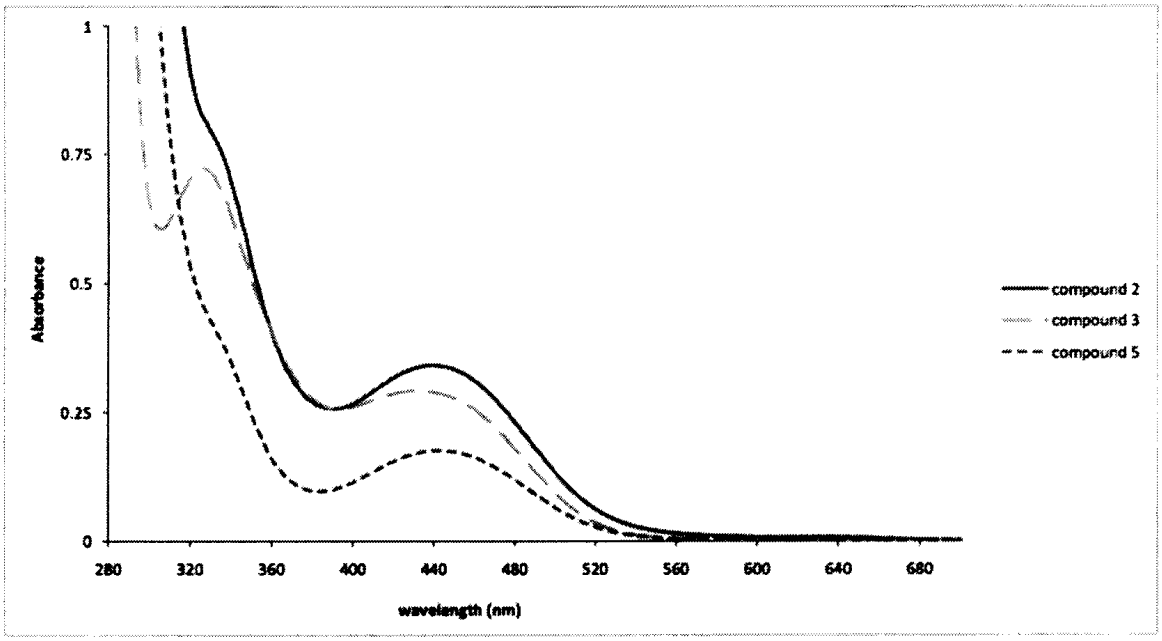

Fig. 2.6 Absorption spectra of 2, 3 and 5 in CH_2Cl_2

2.3.2.3 Infrared Spectroscopy

IR spectroscopy was used for the identification of amide and ester functional groups in the synthesised ferrocenyl complexes. Three characteristic amide peaks are present in the IR spectra of **2** and **5**. These peaks are at 3294 cm^{-1} (N-H stretching), 1654 cm^{-1} (C=O stretching + N-H bending + C-N stretching), 1560 cm^{-1} (N-H bending + C-N stretching) for **2** and at 3277 cm^{-1} (N-H stretching), 1675 cm^{-1} (C=O stretching + N-H bending + C-N stretching), 1573 cm^{-1} (N-H bending + C-N stretching) for **5**. These assignments were completed according to values reported for other ferrocenyl amides.[13] The IR spectrum of **3** displays 3 characteristic peaks for the ester functional group at 1734 cm^{-1} (C=O stretching), 1176 and 1243 cm^{-1} (C-O stretching).

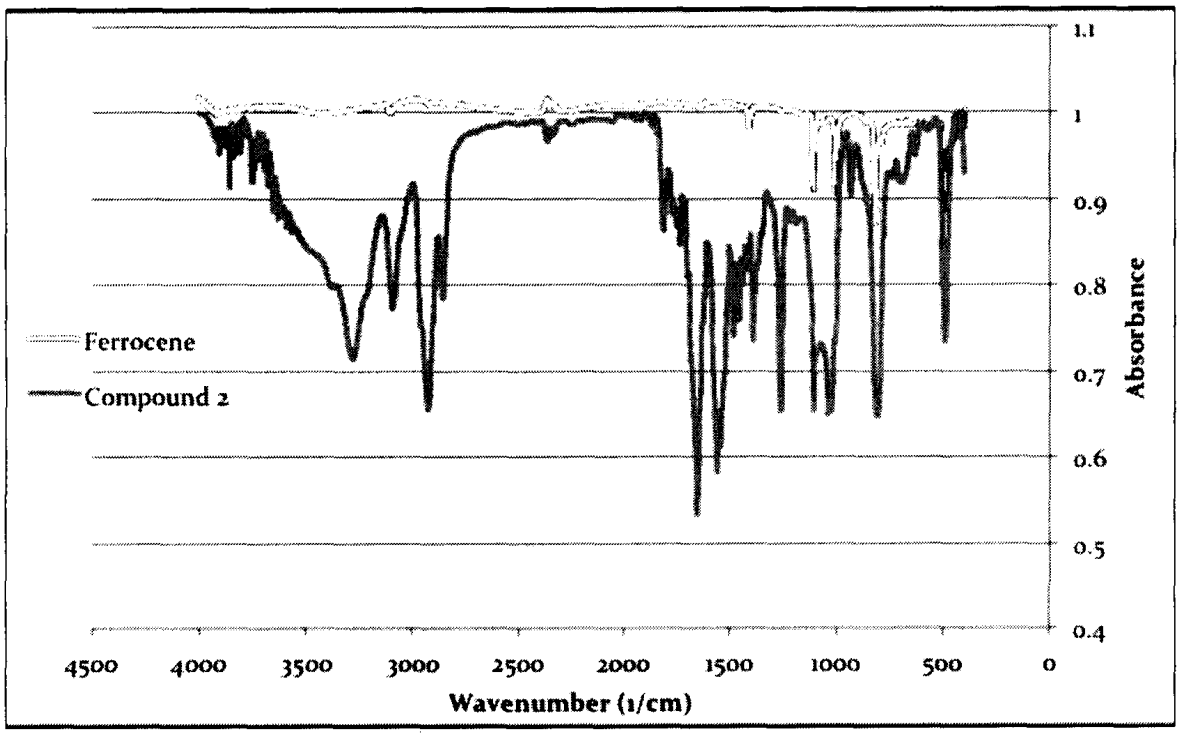

Fig. 2.7 IR spectra of **2** and ferrocene

2.3.2.4 Cyclic Voltammetry

Cyclic voltammetric measurements on dilute (0.5 mM) solutions of 2 and 3 were performed using a 3-electrode system, with glassy carbon working electrode, platinum flag counter electrode, and a silver wire reference electrode in CH_2Cl_2 with $[NBu_4][PF_6]$ (0.1 M) as the supporting electrolyte. The potentials are reported versus S.C.E. and were referenced internally to ferrocene (475 mV)[16], added at the end of the experiments. Voltammograms of 2 and 3 are displayed in Fig 2.8 and Fig 2.9, respectively. Both 2 and 3 show two oxidation peaks in their voltammograms, with one of them being reversible and the other one quasi-reversible. The reversible peaks are assigned to the oxidation of the ferrocenyl moiety in these compounds. 2 shows a reversible oxidation peak at $E_{1/2}$ of 377 mV with $\Delta E = |E_{pa}-E_{pc}| = 45$ mV at a scan rate of 100 mVs^{-1} and i_{pa}/i_{pc} is 0.96 for this peak. The first oxidation peak appears at $E_{1/2} = 507$ mV for 3 with $\Delta E = 50$ mV and i_{pa}/i_{pc} of 1.1. The theoretical ΔE for a one electron oxidation process is 59 mV,[22] which is close to the values found for 2 and 3. The ratio of i_{pa}/i_{pc} for the above mentioned oxidation processes is close to the ideal value for a reversible oxidation peak (1.0). The one electron quasi-reversible peak at $E_{1/2}$ of 1189 mV for 2 and 1102 for 3 is assigned to the oxidation of dithiolane moiety.[23]

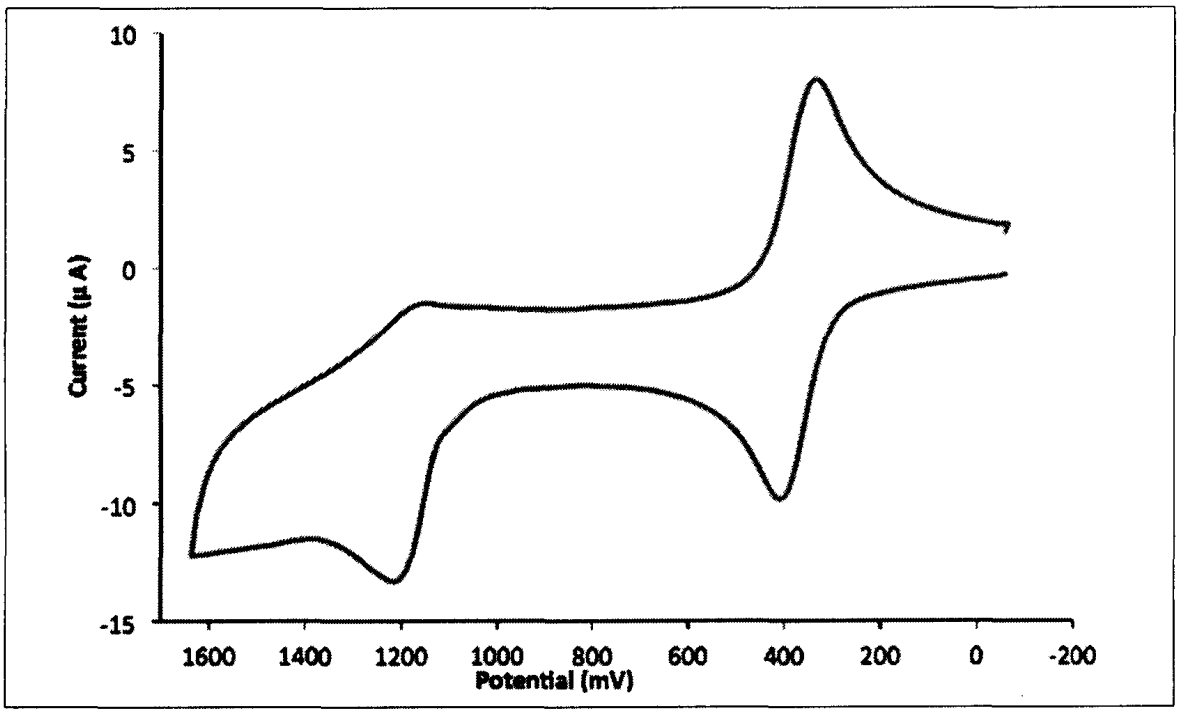

Fig. 2.8 Cyclic voltammogram of **2** in CH_2Cl_2 with 0.1 M $[NBu_4][PF_6]$ at a scan rate of 100 mVs^{-1}.The peak potentials are referenced to S.C.E.

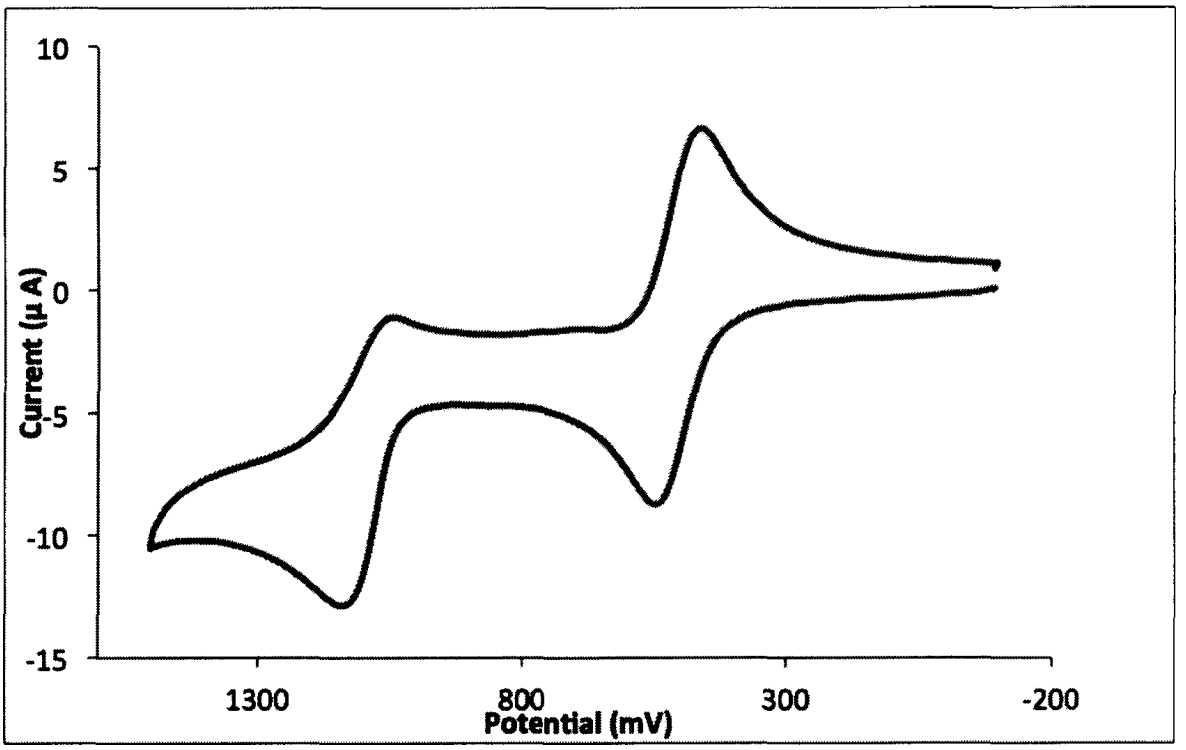

Fig. 2.9 Cyclic voltammogram of **3** in CH_2Cl_2 with 0.1 M $[NBu_4][PF_6]$ at a scan rate of 100 mVs^{-1}.The peak potentials are referenced to S.C.E.

2.3.2.5 X-ray Crystallography

Orange crystals of **2** were obtained by recrystallization from CH_2Cl_2/heptane, and the structure determined using single crystal X-ray diffraction techniques. Complex **2** crystalizes in the non-centrosymmetric, orthorhombic space group Pca2(1) with 8 molecules in the unit cell (Z=8). There are two independent molecules in the asymmetric unit. Due to the size of the crystals, the weak nature of the data and crystallographic disorder of one of the C_3S_2 rings, there is some uncertainty associated with the refinement. A summary of the pertinent bond lengths and angles for molecule 1, which displays no site disorder, is listed in Table 2.1. The S-S bond length in **2** is 2.029(6) Å, slightly shorter than S-S bond in Lipoic acid (2.053(4)).[24] The Cp rings are almost perfectly parallel. The molecular structure of **2** is shown in Fig. 2.9. (molecule 1)

Table 2.1 Selected bond lengths [Å] and angles [°] for **2** (molecule 1)

Fe(11)-C(11)	2.033(6)
N(11)-C(11)	1.426(7)
O(11)-C(111)	1.225(7)
S(11)-S(21)	2.016(4)
C(161)-S(11)-S(21)	97.6(3)
C(181)-S(21)-S(11)	95.3(5)

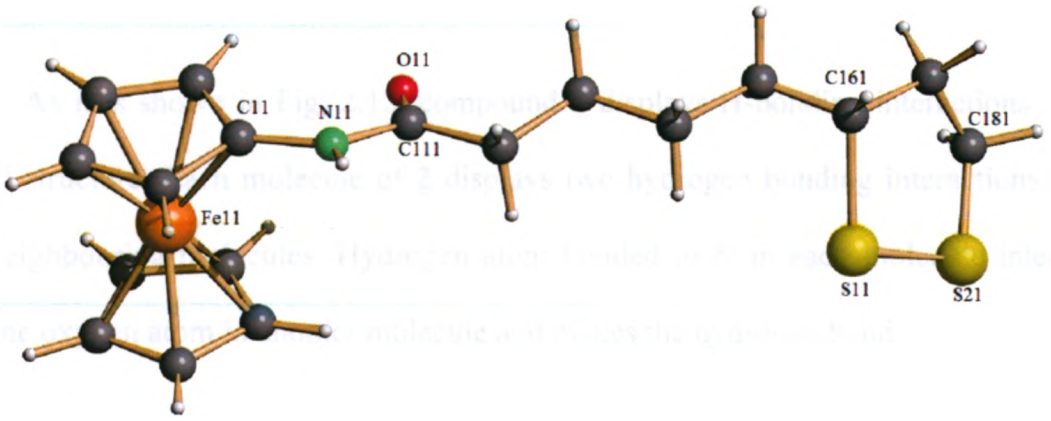

Fig. 2.10 The molecular structure of **2** (molecule 1)

Fig. 2.11 illustrates the molecular structure of **2** with a site disorder of the C_3S_2 ring (molecule 2). The two distorted rings are shown in different colors (purple and yellow). The purple ring was refined with a partial occupancy of 67% in the structure, with 33% of occupancy for the yellow ring. The two sites however have opposite configuration of the chiral methyne centre in the C_3S_2 ring. There is also uncertainty assigned to the S/C positions of these rings. Ultimately, stronger diffraction data will be required to resolve the disorder more completely.

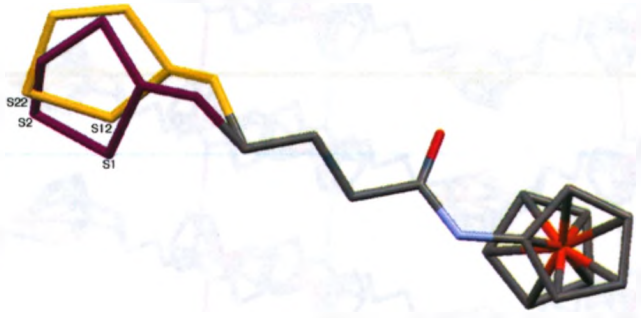

Fig. 2.11 The molecular structure of **2** (disorder in C_3S_2 ring)

As it is shown in Fig. 2.12, compound **2** displays H-bonding interactions in its crystal structure. Each molecule of **2** displays two hydrogen bonding interactions with two neighbouring molecules. Hydrogen atom bonded to N in each molecule interacts with the oxygen atom in another molecule and makes the hydrogen bond.

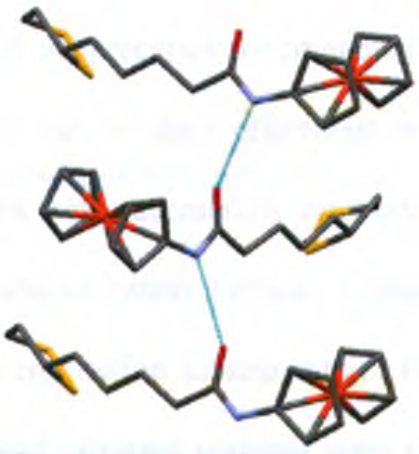

Fig. 2.12 Molecular structure of **2** with hydrogen bonding interactions.

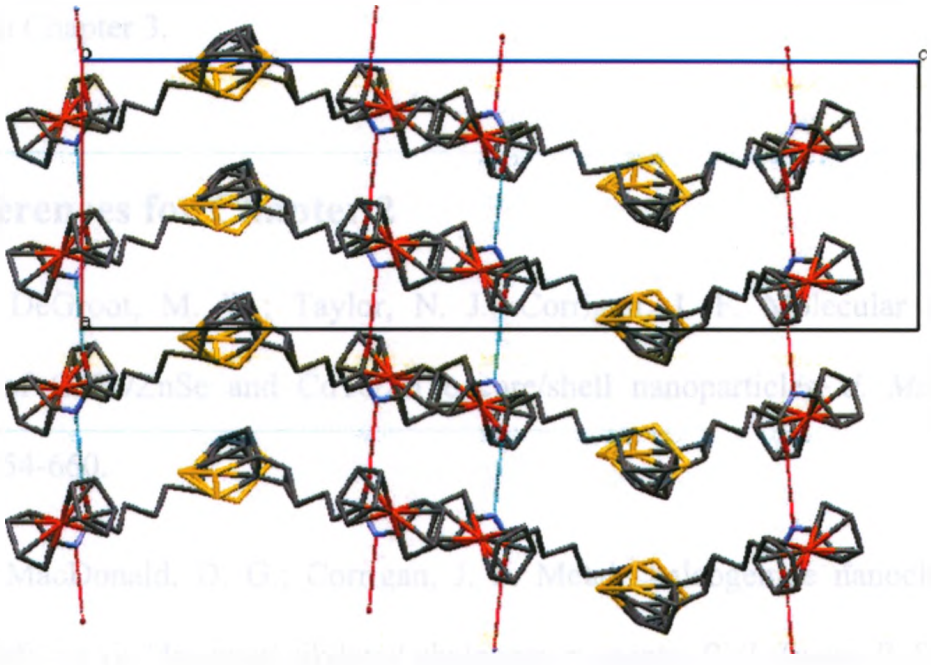

Fig. 2.13 The packing arrangement of **2**. Hydrogen atoms have been omitted for clarity.

2.4 Conclusion

The successful synthesis of ferrocene based dithiolate ligands was a challenging one due to the sensitivity of the S-S bond in these compounds and the formation of insoluble polymers when compounds are exposed to light or heat. Even by completing the reactions in the dark, the acylation of ferrocene to yield **4** and the synthesis of 2-(1, 2-dithiolan-3-yl)acetic acid, the precursor for compound **5**, had such low yields such that the subsequent steps could not be done effectively with these approaches. Ferrocene based dithiolane complexes were successfully synthesized and fully characterized using different spectroscopic characterization methods. Compounds **2** and **3** were synthesized in high yields and these were used in subsequent reactions. To use these complexes for cluster assembly, the related silylated reagents were prepared. Complexation of these ligands with Pt, the formation of silylated reagents and their use in cluster assembly are discussed in Chapter 3.

2.5 References for Chapter 2

(1) DeGroot, M. W.; Taylor, N. J.; Corrigan, J. F. Molecular nanocluster analogues of CdSe/ZnSe and CdTe/ZnTe core/shell nanoparticles. *J. Mater. Chem.* **2004**, *14*, 654-660.

(2) MacDonald, D. G.; Corrigan, J. F. Metal chalcogenide nanoclusters with 'tailored' surfaces via 'designer' silylated chalcogen reagents. *Phil. Trans. R. Soc. A* **2010**, *368*, 1455-1472.

(3) Stepnicka, P. In *Ferrocenes :ligands, materials and biomolecules;* J.Wiley: Chichester, England; Hoboken, NJ, 2008; , pp 655.

(4) Astruc, D.; Ornelas, C.; Ruiz Aranzaes, J. Ferrocenyl-terminated dendrimers: Design for applications in molecular electronics, molecular recognition and catalysis. *J. Inorg. Organomet. Polym.* **2008**, *18*, 4-17.

(5) Whittell, G. R.; Manners, I. Metallopolymers: New multifunctional materials. *Adv. Mater.* **2007**, *19*, 3439-3468.

(6) Wolfe, R. L.; Balasubramanian, R.; Tracy, J. B.; Murray, R. W. Fully ferrocenated hexanethiolate monolayer-protected gold clusters. *Langmuir* **2007**, *23*, 2247-2254.

(7) Ghosh, K.; Zhao, Y.; Yang, H. B.; Northrop, B. H.; White, H. S.; Stang, P. J. Synthesis of a new family of hexakisferrocenyl hexagons and their electrochemical behavior. *J. Org. Chem.* **2008**, *73*, 8553-8557.

(8) Labande, A.; Ruiz, J.; Astruc, D. Supramolecular gold nanoparticles for the redox recognition of oxoanions: Syntheses, titrations, stereoelectronic effects, and selectivity. *J. Am. Chem. Soc.* **2002**, *124*, 1782-1789.

(9) Mulrooney, R. C.; Singh, N.; Kaur, N.; Callan, J. F. An "off-on" sensor for fluoride using luminescent CdSe/ZnS quantum dots. *Chem. Commun.* **2009**, 686-688.

(10) Wallbank, A. I.; Corrigan, J. F. 1,1 '-Bis(trimethylsilylseleno)ferrocene in cluster synthesis: a redox active surface on a copper-selenide core. *Chem. Commun.* **2001**, 377-378.

(11) Lebold, T. P.; Stringle, D. L. B.; Workentin, M. S.; Corrigan, J. F. Functionalizing the surface of II-VI clusters: redox active centres on the adamantoid complex $[Cd_4Cl_4\{\mu\text{-}(SeC_5H_4)Fe(C_5H_5)\}_6]^{2-}$ *Chem. Commun.* **2003**, 1398-1399.

(12) Astruc, D.; Daniel, M. C.; Ruiz, J. Dendrimers and gold nanoparticles as exo-receptors sensing biologically important anions. *Chem. Commun.* **2004**, 2637-2649.

(13) Heinze, K.; Schlenker, M. Main chain ferrocenyl amides from 1-aminoferrocene-1′-carboxylic acid. *Eur. J. Inorg. Chem.* **2004**, 2974-2988.

(14) Davis, W. L.; Shago, R. F.; Langner, E. H. G.; Swarts, J. C. Synthesis and electrochemical properties of a series of ferrocene-containing alcohols. *Polyhedron* **2005**, *24*, 1611-1616.

(15) Chen, Y. S.; Lawton, R. G. An efficient synthetic route to 2-(1,2-dithiolan-3-yl)acetic acid. Trisnorlipoic acid and amide derivatives. *Tetrahedron Lett.* **1997**, *38*, 5785-5788.

(16) Aranzaes, J. R.; Daniel, M. C.; Astruc, D. Metallocenes as references for the determination of redox potentials by cyclic voltammetry - Permethylated iron and cobalt sandwich complexes, inhibition by polyamine dendrimers, and the role of hydroxy-containing ferrocenes. *Can. J. Chem.* **2006**, *84*, 288-299.

(17) Barltrop, J. A.; Hayes, P. M.; Calvin, M. The chemistry of 1,2-dithiolane (trimethylene disulfide) as a model for the primary quantum conversion act in photosynthesis. *J. Am. Chem. Soc.* **1954**, *76*, 4348-4367.

(18) Clayden, J.; Greeves, N.; Warren, S.; Wothers, P. In *Organic Chemistry;* Oxford University Press: Oxford, 2001.

(19) Rogers, R. S. A General-Synthesis of Phosphonic acid dichlorides using oxalyl chloride and DMF catalysis. *Tetrahedron Lett.* **1992**, *33*, 7473-7474.

(20) Ihre, H.; Hult, A.; Soderlind, E. Synthesis, characterization, and H-1 NMR self-diffusion studies of dendritic aliphatic polyesters based on 2,2-bis(hydroxymethyl)propionic acid and 1,1,1-tris(hydroxyphenyl)ethane. *J. Am. Chem. Soc.* **1996**, *118*, 6388-6395.

(21) Bergson, G.; Schotte, L.; Claeson, G. Ultraviolet absorption spectra of saturated disulphides and diselenides. *Acta Chem. Scand.* **1962**, *16*, 1159-1174.

(22) Kissinger, P. T.; Heineman, W. R. Cyclic voltammetry. *J. Chem. Educ.* **1983**, *60*, 702-706.

(23) Corduneanu, O.; Garnett, M.; Brett, A. M. O. Anodic oxidation of alpha-lipoic acid at a glassy carbon electrode and its determination in dietary supplements. *Anal. Lett.* **2007**, *40*, 1763-1778.

(24) Stroud, R. M.; Carlisle, C. H. Single-crystal structure determination of dl-6-thioctic acid, $C_8H_{14}O_2S_2$. *Acta Crystallogr. Sect. B-Struct. Sci.* **1972**, *B 28*, 304-306.

3 Complexation with Pt and Synthesis of Silylated Reagents

3.1 Introduction

A powerful method for chalcogen delivery in the synthesis of nanometre-sized metal–chalcogen clusters is usage of silylated chalcogen reagents. Compared to other methods such as the use of alkali metal-chalcogenides (A_2E) or H_2E, silylated chalcogen reagents present a more handleable source of chalcogen under milder reaction conditions.

$$M\text{-}X_n + n\ RESiMe_3 \rightarrow [M(ER)_n]_m + n\ X\text{-}SiMe_3 \quad 3.1$$

$$M\text{-}X_n + n/2\ E(SiMe_3)_2 \rightarrow (ME_{n/2})_2 + n\ X\text{-}SiMe_3 \quad 3.2$$

$$M\text{-}X_n + n/2\ RESiMe_3 + n/4\ E(SiMe_3)_2 \rightarrow [M(ER)_{n/2}E_{n/4}]_m + n\ X\text{-}SiMe_3 \quad 3.3$$

The formation of an X–Si bond and elimination of X–$SiMe_3$ (X=halide, OAc, alkyl, etc.) is the driving force for these reactions.[1] Silylated chalcogen reagents also give us this opportunity to tune the R group of the ligand easily and they can be tailored to introduce specific chemical functionalities into the cluster such as ferrocenyl units.[2, 3]

Before cluster assembly studies, to test the reactivity of compounds **2** and **3**, the oxidative addition of their S-S bond to zero-valent platinum was targeted. One of the significant features of disulfide redox chemistry is the oxidative addition of the S-S bond to low-valent metal centers such as platinum(0) that have an important role in different areas such as medicinal chemistry and transition metal catalysis.[4-6] Deviation from ideal C-S-S-C torsion angle (90°) increases the reactivity of the S-S bond.[7, 8] This deviation,

which can be caused by steric interference or ring closure, correlates with the elongation of the S-S bond.[9] During our investigations on the preparation of ligands **2** and **3** (see Chapter 2), we targeted the coordination complexes *cis*-$Pt(PPh_3)_2(C_{18}H_{23}FeNOS_2)$ (**6**) and *cis*-$Pt(PPh_3)_2(C_{19}H_{24}FeO_2S_2)$ (**7**).

Herein, we describe the complexation of ferrocene based dithiolate ligands (**2** and **3**) to platinum using the oxidative addition of the S-S bonds in these compounds to Pt(0). The preparation of silylated reagents, $C_{24}H_{41}FeNOS_2Si_2$ (**9**) and $C_{25}H_{42}FeO_2S_2Si_2$ (**11**) from considered ligands (**2** and **3**) is also presented.

3.2 Experimental

3.2.1 General Synthetic Techniques and Starting Materials

All syntheses were performed under a dinitrogen atmosphere using standard Schlenk line and glove box techniques unless otherwise stated. All chemicals were used as received from Strem Chemicals and/or Aldrich. Tetrahydrofuran, diethyl ether, hexanes, and pentane purchased from Caledon were dried by passing through packed columns of activated alumina using a commercially available MBraun MB-SP Series solvent purification system. Dichloromethane, chloroform and chloroform-d were purchased from Caledon, and distilled over P_2O_5. $Pt(PPh_3)_4$ was prepared using a published procedure.[10]

^1H, $^{31}P\{^1H\}$ and $^{13}C\{^1H\}$ NMR spectra were obtained on a Varian Mercury 400 MHz spectrometer and are reported in ppm. These spectra were referenced internally to solvent peaks relative to $SiMe_4$ at δ=0 ppm.

Single crystal X-ray diffraction measurement was performed on a Bruker APEXII diffractometer, with the molecular structures determined via direct methods using the SHELX suite of crystallographic programs (G.M. Sheldrick, Madison, WI). A BAS 100 electrochemical workstation using a 3-electrode system, with glassy carbon working electrode, platinum flag counter electrode, and a silver wire reference electrode with 0.1 M $[NBu_4][BF_4]$ in CH_2Cl_2 as the supporting electrolyte was used for electrochemical measurements. The potentials are reported versus a saturated calomel electrode (S.C.E.) and were referenced internally to ferrocene (475 mV),[11] added at the end of the experiments. Ultraviolet-visible (UV-Vis) absorption spectra were recorded on a Varian Cary 300 Bio UV-Vis spectrophotometer in CH_2Cl_2.

3.2.2 *cis*-(*N*-ferrocenyl-*rac*-6, 8-dithiolatooctaneamide) bis(triphenylphosphine)platinum(II) (6):

0.20 g of $Pt(PPh_3)_4$ (0.16 mmol) was dissolved in 15 ml of benzene. 0.066 g of 2 (0.16 mmol) was added to the solution. 2 was completely dissolved after about 10 minutes of stirring. The progress of the reaction was monitored by NMR spectroscopy. ^1H and ^{31}P NMR spectra indicated that the reaction was complete after 20 hours. The product was isolated by adding ~ 15 ml of pentane and removing the mother liquor from the purified product. The dark orange solid was dissolved in a mixture of $CHCl_3$ and pentane (2:2.5) and cooled to -25 °C to yield single crystals suitable for X-ray diffraction analysis. Yield = 47%

^1H NMR (400 MHz, $CDCl_3$, 23 °C) δ = 7.47 (t, $^3J_{HH}$=7.6 Hz, 6H), 7.41 (t, $^3J_{HH}$=7.6 Hz, 6H), 7.24 (m, 6H), 7.14 (t, $^3J_{HH}$=7.6 Hz, 6H), 7.09 (t, $^3J_{HH}$=7.6 Hz, 6H), 6.55 (s,

1H), 4.61 (s, 1H), 4.57 (s, 1H), 4.14 (s, 5H), 3.97 (s, 2H), 3.34 (m, 2H), 2.89 (m, 1H), 2.14 (m, 1H), 2.10 (t, $^{3}J_{HH}$=7.8 Hz, 2H), 1.68 (m, 1H), 1.56 (m, 2H), 1.34 (m, 4H). $^{13}C\{^{1}H\}$ NMR (100.5 MHz, CDCl3) δ = 171.56 (C(O)), 134.78 (CH), 130.03 (CH), 127.49 (CH), 94.80 (CN), 69.06 (Cp), 64.21 (CH), 61.32 (CH), 39.63 (CHS), 38.73 (CH_2), 37.41 (CH_2S), 27.54 (CH_2), 26.00 (CH_2), 25.30 (CH_2), 24.51 (CH_2). $^{31}P\{^{1}H\}$ NMR ($CDCl_3$, 23 °C) δ = 24.78 (dd, $^{2}J_{PP}$=21.0 Hz, $^{1}J_{PPt}$=2865 Hz), 22.81 (dd, $^{2}J_{PP}$=21.0 Hz, $^{1}J_{PPt}$=2804 Hz). HRMS: Calcd for $C_{54}H_{53}FeNOP_2PtS_2$ (*m/z*): 1108.2041 Found: 1108.2038. Anal. Calc. (%) for $C_{54}H_{53}FeNOP_2PtS_2$: C 58.47, H 4.82, N 1.26, S 5.77. Found: C 57.30, H 4.51, N 1.11, S 4.89.

3.2.3 *cis*-(ferrocenemethyl *rac*-6, 8-dithiolatooctanoate) bis(triphenylphosphine)platinum(II) (7):

$Pt(PPh_3)_4$ (0.20 g, 0.16 mmol) was dissolved in 15 ml of benzene. Compound 3 (0.65 g, 0.16 mmol) was added to the solution. It was stirred at room temperature for 20 hours and NMR spectroscopy confirmed the completion of the reaction. The product was purified by washing with pentane several times to yield 7 as a dark brown oil. Yield = 51%

^{1}H NMR (400 MHz, $CDCl_3$, 23 °C) δ = 7.52-7.08 (m, 60H(due to some impurities and overlapping with solvent peak)), 4.88 (s, 2H), 4.27 (vt, J_{HH}=1.8 Hz, 2H), 4.17 (vt, J_{HH}=1.9 Hz, 2H), 4.16 (s, 5H), 3.30 (m, 2H), 2.88 (m, 1H), 2.18 (t, $^{3}J_{HH}$=7.8 Hz, 2H), 2.11 (m, 1H), 1.64 (m, 1H), 1.49 (m, 2H), 1.30 (m, 4H). $^{31}P\{^{1}H\}$ NMR ($CDCl_3$, 23 °C) δ = 24.91 (dd, $^{2}J_{PP}$=21.0 Hz, $^{1}J_{PPt}$=2860 Hz), 22.83 (dd, $^{2}J_{PP}$=21.0 Hz, $^{1}J_{PPt}$=2801 Hz).

3.2.4 *N*-ferrocenyl-*rac*-6, 8-dithioloctaneamide (8):

The orange-brown solid $C_{18}H_{23}FeNOS_2$ (2) (0.15 g, 0.38 mmol) was dissolved in 10 ml of THF and a degassed solution of $NaBH_4$ (0.029 g, 0.77 mmol) in 4 ml of water was added. The solution was stirred at room temperature for 2 hours. 1M HCl (0.77 ml, 0.77 mmol) was then added and the solution was stirred for 15 min. The solution was diluted with 20 ml of degassed water and extracted with dichloromethane (2×20 ml). The organic layers were combined, dried over $MgSO_4$ and the solvent was evaporated *in vacuo* to yield 8 as an orange oil. Yield=81%

^{1}H NMR (400 MHz, $CDCl_3$, 23 °C) δ = 6.46 (br.s, 1H), 4.61 (br.s, 2H), 4.16 (s, 5H), 4.02 (vt, J_{HH}=1.8 Hz, 2H), 2.94 (m, 1H), 2.75-2.65 (m, 2H), 2.24 (t, $^3J_{HH}$=7.4 Hz, 2H), 1.88 (m, 1H), 1.76-1.65 (m, 4H), 1.60-1.48 (m, 3H), 1.34 (t, $^3J_{HH}$=7.9 Hz, 1H), 1.30 (d, $^3J_{HH}$=8.2 Hz, 1H). ^{13}C{^{1}H} NMR (100.5 MHz, CDCl3) δ = 170.80 (C(O)), 94.54 (CN), 69.17 (Cp), 64.54 (CH), 61.38 (CH), 42.80 (CHS), 41.75 (CH_2), 39.34 (CH_2S), 38.75 (CH_2), 37.09 (CH_2), 26.63 (CH_2), 25.22 (CH_2). HRMS: Calcd for $C_{18}H_{25}ONS_2Fe$ (*m/z*): 391.0727 Found: 391.0716.

3.2.5 *N*-ferrocenyl-*rac*-6, 8-trimethylsilylsulfooctanamide (9):

$ClSiMe_3$ (0.15 ml, 1.15 mmol) was added to a stirred solution of $C_{18}H_{25}FeNOS_2$ (8) (0.11 g, 0.30 mmol) which was dissolved in 15 ml of CH_2Cl_2 with NEt_3 (0.16 ml, 1.15 mmol) at 0 °C. The solution was stirred at 0 °C for 15 min and at room temperature for 3 hours. 20 ml of heptane was added and the CH_2Cl_2 was removed under vacuum. The heptane solution was filtered and the solvent was evaporated *in vacuo* to yield compound 9 as an orange oil. Yield=90%.

^{1}H NMR (400 MHz, $CDCl_3$, 23 °C) δ = 6.53 (br s, 1H), 4.57 (m, 2H), 4.14 (s, 5H), 3.98 (vt, J_{HH}=2.0 Hz, 2H), 3.55 (m, 1H), 2.86 (m, 2H), 2.61 (m, 3H), 2.23 (t, $^3J_{HH}$=7.6 Hz, 2H), 1.86 (m, 1H), 1.68 (m, 2H), 1.52 (m, 2H), 0.31(s, 9H), 0.30(s, 13H(due to some impurities)). $^{13}C\{^1H\}$ NMR (100.5 MHz, $CDCl_3$) δ = 109.99 (CN), 69.12 (Cp), 64.47 (CH), 62.58(CH), 61.38 (CHS), 41.39 (CH_2), 38.18 (CH_2S), 37.21 (CH_2), 32.65 (CH_2), 26.35 (CH_2), 25.57 (CH_2), 1.67 (CH_3), 0.99 (CH_3). HRMS: Calcd for $C_{24}H_{41}FeNOS_2Si_2$ (*m/z*): 535.1517 Found: 535.1525.

3.2.6 Ferrocenemethyl *rac*-6, 8-dithioloctanoate (10):

The orange oil $C_{19}H_{24}FeO_2S_2$ (3) (0.15 g, 0.38 mmol) was dissolved in 10 ml of THF and a degassed solution of $NaBH_4$ (0.029 g, 0.77 mmol) in 4 ml of water was added. The solution was stirred at room temperature for 2 hours. 1M HCl (0.77 ml, 0.77 mmol) was then added and the solution was stirred for 15 min. The solution was diluted with 20 ml of degassed water and extracted with dichloromethane (2×20 ml). The organic layers were combined, dried over $MgSO_4$ and the solvent was evaporated *in vacuo* to yield **10** as an orange oil. Yield=64%.

^{1}H NMR (400 MHz, $CDCl_3$, 23 °C) δ = 4.89 (s, 2H), 4.26 (vt, J_{HH}=2.0 Hz, 2H), 4.17 (vt, J_{HH}=1.8 Hz, 2H), 4.15 (s, 5H), 2.89 (m, 1H), 2.74-2.64 (m, 2H), 2.29 (t, $^3J_{HH}$=7.3 Hz, 2H), 1.88 (m, 1H), 1.61-1.73 (m, 4H), 1.55-1.45 (m, 3H), 1.33 (t, $^3J_{HH}$=8.2 Hz, 1H), 1.27 (d, $^3J_{HH}$=7.6 Hz, 1H). HRMS: Calcd for $C_{19}H_{26}O_2S_2Fe$ (*m/z*): 406.0724 Found: 406.0735.

3.2.7 Ferrocenemethyl *rac*-6, 8-trimethylsilylsulfooctanoate (11):

$ClSiMe_3$ (0.15 ml, 1.15 mmol) was added to a stirred solution of $C_{19}H_{26}FeO_2S_2$ (**10**) (0.12 g, 0.30 mmol) dissolved in 15 ml of CH_2Cl_2 with NEt_3 (0.16 ml, 1.15 mmol) at 0 °C. The solution was stirred at 0 °C for 15 min and at room temperature for 3 hours. 20 ml of heptane was added and the CH_2Cl_2 was removed under vacuum. The heptane solution was filtered and the solvent was evaporated *in vacuo* to yield compound **11** as an orange oil. Yield=82.%

^1H NMR ($CDCl_3$, 23°C) δ = 4.88 (s, 2H), 4.25 (vt, J_{HH}=1.8Hz, 2H), 4.16 (vt, J_{HH}=1.8 Hz, 2H), 4.15 (s, 5H), 2.82 (m, 1H), 2.60 (m, 2H), 2.28 (t, $^3J_{HH}$=7.2 Hz, 2H), 1.78 (m, 2H), 1.60 (m, 4H), 1.41 (m, 2H), 0.31 (s, 9H), 0.30 (s, 9H). HRMS: Calcd for $C_{25}H_{42}FeO_2S_2Si_2$ (*m/z*): 550.1514Found: 550.1520.

3.2.8 Reaction of 9 with silver acetate (12):

5 ml of THF was added to silver acetate (0.136 g, 0.82 mmol) followed by tri-n-propylphosphine (0.20 ml, 1.0 mmol) to dissolve it. This solution was cooled to -70 °C and $C_{24}H_{41}FeNOS_2Si_2$ (**9**) (0.22 g, 0.41 mmol) in 5 ml of THF was added. The solution was stirred until it reached room temperature, then for 2 hours at room temperature. The progress of the reaction was followed by ^1H NMR spectroscopy. According to ^1H NMR spectra the reaction was complete after 2 hours. The product was purified by several washings with pentane.

3.3 Results and Discussion

3.3.1 Synthesis

An example of the oxidative addition of a disulfide linkage to Pt(0) was reported in 1964 by Davison *et al.* for the first time[12] and this is now a well developed strategy for the complexation of thiolate ligands onto electron rich metal centers. More recently, Weigand and co-workers published the reaction of a 1,2-dithiolane derivative with a Pt(0) source leading to the *cis* mononuclear complex of platinum [$(Ph_3P)_2Pt(-S-CH_2-CHPh-CH_2-S-)$].[13] Considering the published procedures for oxidative addition of disulfides to zero-valent platinum[6, 14] we successfully targeted reactions of the disulfide complexes **2** and **3** with platinum. The oxidative addition of **2** and **3** to Pt(0) (Scheme 3.1 and Scheme 3.2, respectively) was done by dissolving $Pt(PPh_3)_4$ in benzene followed by the addition of the ferrocenyl reagents. The progress of these reactions was easily followed by NMR spectroscopy, which indicated the reactions were complete after ~20 hours of stirring at room temperature.

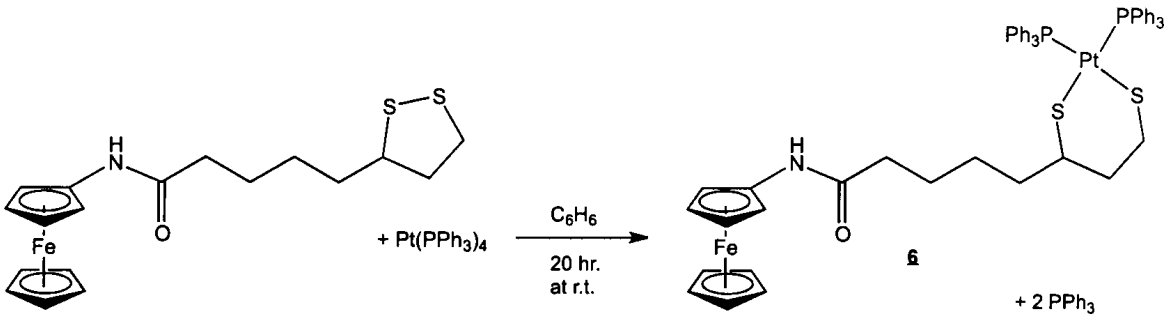

Scheme 3.1 Oxidative addition of **2** to Pt(0)

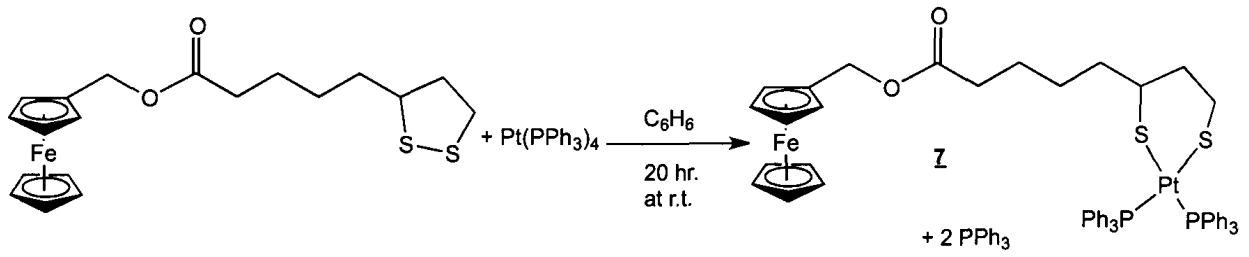

Scheme 3.2 Oxidative addition of 3 to Pt(0)

The reduction of the disulfide linkage in 2 and 3 can be done with $NaBH_4$ to yield the corresponding dithiols after acidic work-up. The formation of dithiols **8** and **10** was confirmed by the appearance of peaks assigned to -SH at ~1.30 ppm in their ^1H NMR spectra. The dithiols could then be reacted with $ClSiMe_3$ in the presence of base to yield the corresponding silylated reagents **9** and **11**, respectively. These reactions are illustrated in the schemes below.

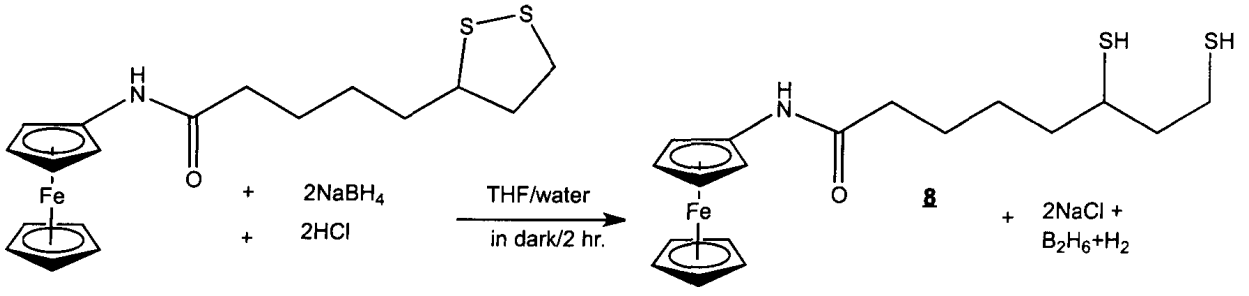

Scheme 3.3 Reduction of 2 and formation of 8

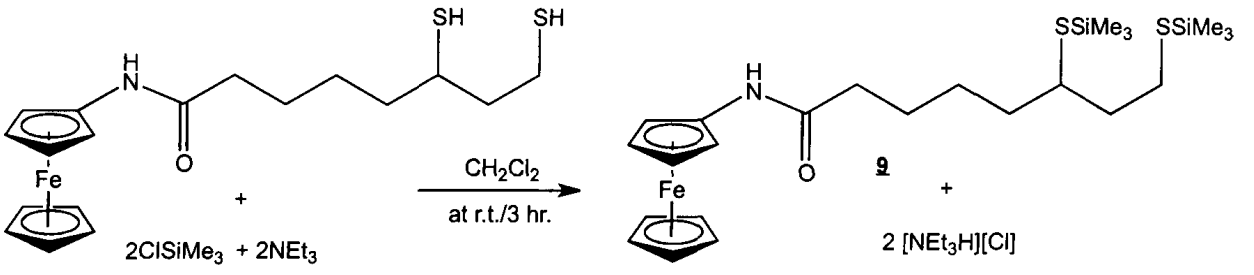

Scheme 3.4 Synthesis of 9

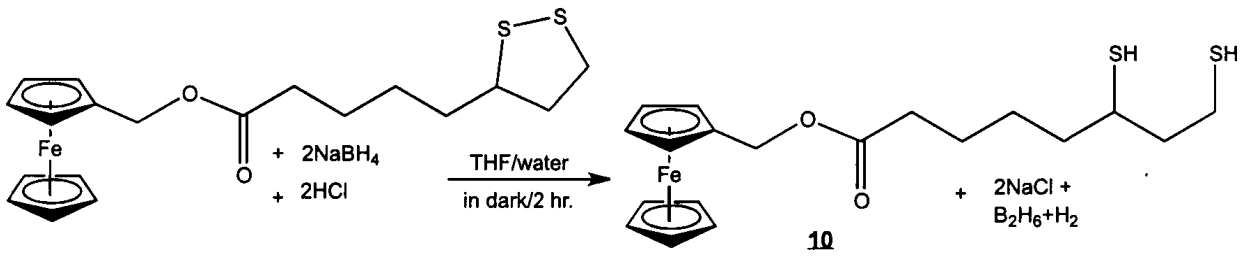

10

Scheme 3.5 Reduction of 3 and formation of 10

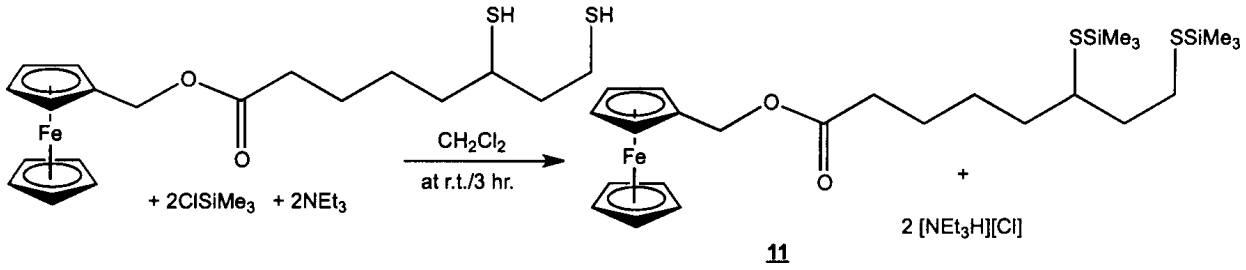

11

Scheme 3.6 Synthesis of 11

Several reactions were probed between 9 or 10 and the silver (I) complexes AgOAc and $AgNO_3$. Different phosphines such as triphenylphosphine, tri-n-butylphosphine and tri-n-propylphosphine were used to solubilize silver salts, which seem to have an effect on the nature of the final products according to observations (color, solubility...). Unfortunately no high quality single crystals were obtained from these reactions. Due to the presence of extra phosphines in the reaction products and difficulties in the purification of these complexes, they were not able to be fully characterized. A typical reaction protocal is described in the experimental section. In the described procedure, 9 was reacted with silver acetate solubilized by tri-n-propylphosphine in THF as solvent. The reaction was started at -70 °C and warmed to room temperature gradually. It was anticipated that the reaction proceeds by elimination of $AcOSiMe_3$ and a silver thiolate cluster forms as consequence of the bridging

capability and preference of the thiolate ligands. (Scheme 3.7) ^{1}H NMR spectroscopy confirmed this process. The product (**12**) was washed several times with pentane but unfortunately no high quality crystals were obtained and **12** was characterized utilizing other methods.

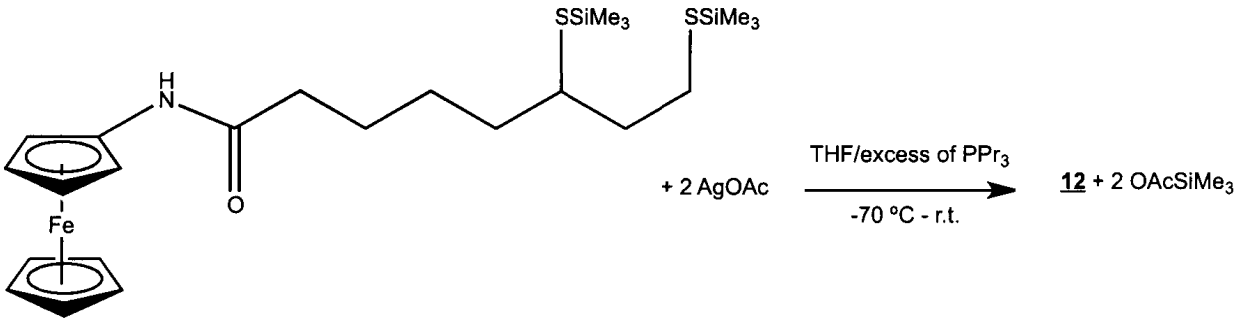

Scheme 3.7 Reaction of **9** with silver acetate

3.3.2 Characterization

3.3.2.1 NMR Spectroscopy

All of the synthesized complexes were characterized by NMR spectroscopy and chemical shift data were obtained at room temperature in $CDCl_3$. ^{31}P NMR spectroscopy was especially useful for confirming the formation of **6** and **7**.

^{1}H and $^{13}C\{^{1}H\}$ NMR spectra of **6** and **7** show similar patterns to the spectra of **2** and **3** with slight shift in the position of the peaks of the ferrocenyl unit in addition to the phenyl hydrogen peaks in aromatic region. The CH peak in C_3S_2 ring shifted its position from 3.58 ppm in the ^{1}HNMR spectrum of **2** to 3.32 ppm in the spectrum of **6**. A similar shift in the corresponding CH resonance (3.52 ppm) was observed in the ^{1}H NMR spectrum of **3** in the spectrum of **7** (3.30 ppm). In the $^{31}P\{^{1}H\}$ NMR spectra of **6** and **7** two peaks are present at ca. 25 and 23 ppm. These peaks display the expected ^{195}Pt

satellites with $^{1}J_{PtP}$ values in the range of 2801 and 2865 Hz and $^{2}J_{PP}$ values of 21 Hz for the two inequivalent phosphorus nuclei. The $^{31}P\{^{1}H\}$ NMR spectrum of **6** is shown in Fig. 3.1. The observed coupling constant values are in close agreement with those reported for related square planar Pt(II) complexes with two *cis*-phosphine ligands *trans* to two ligands with different *trans* influences.[15, 16] Assignment of the two signals to the inequivalent phosphines was not determined.

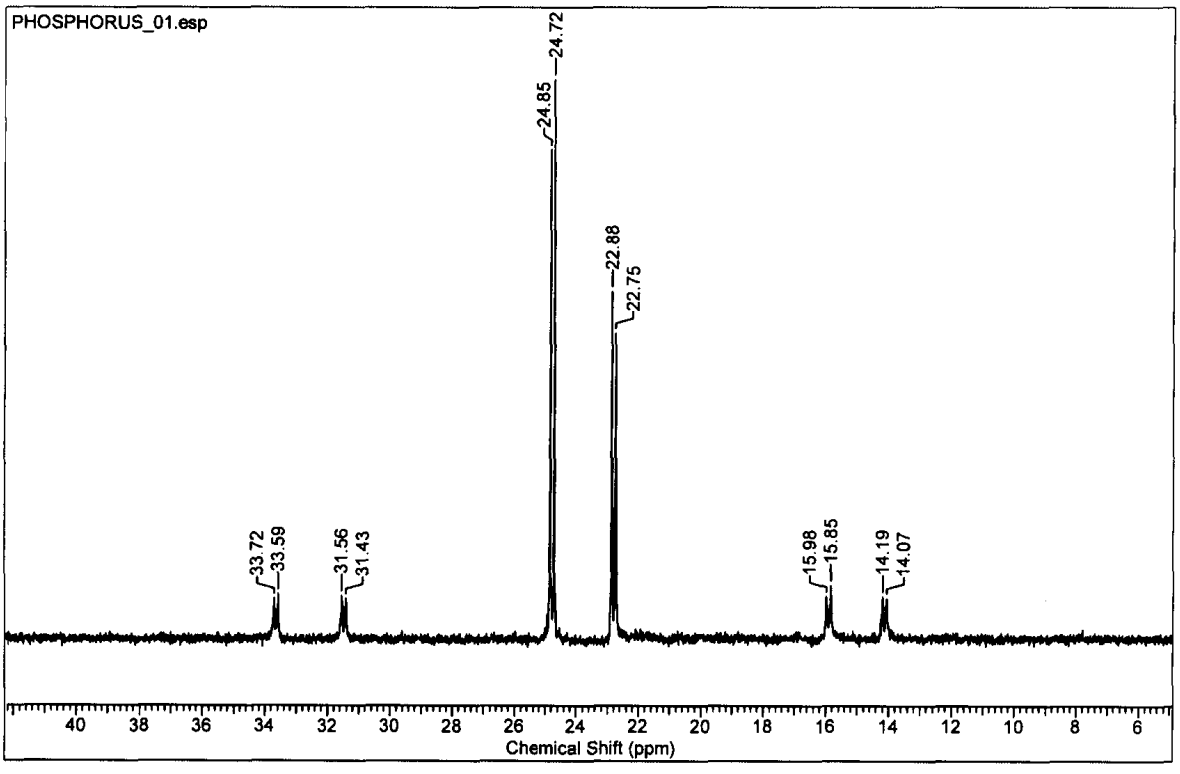

Fig. 3.1 $^{31}P\{^{1}H\}$ NMR spectrum of **6** in $CDCl_3$.

The formation of **8**, **9**, **10** and **11** was also followed by NMR spectroscopy. Formation of the dithiols was confirmed by the appearance of signals assigned to –SH groups. These were observed at 1.34 (t, $^{3}J_{HH}$=7.9 Hz, 1H) and 1.30 (d, $^{3}J_{HH}$=8.2 Hz, 1H) ppm for **8** and at 1.33 (t, $^{3}J_{HH}$=8.2 Hz, 1H) and 1.27 (d, $^{3}J_{HH}$=7.6 Hz, 1H) ppm for **10**.

The proton signals for those H centers closest to the thiols shifted ~ 0.5 ppm to the lower chemical shifts comparing to their position in the ^{1}H NMR spectra of the starting materials (**2** and **3**) upon opening of the C_3S_2 ring. The position of –CH signal in the C_3S_2 ring was the most shifted, from 3.58 ppm in the ^{1}H NMR spectrum of **2** to 2.94 ppm for **8** and, similarly, from 3.52 ppm in the ^{1}H NMR spectrum of **3** to 2.89 ppm for **10**. After reaction of the dithiols with $ClSiMe_3$ in the presence of Et_3N, the signals for the thiol peaks were replaced with 2 peaks centered around ~0.3 ppm assigned to –$SSiMe_3$. The ^{1}H NMR spectra of **8** and **9** are shown in Fig. 3.2 and Fig. 3.3, respectively.

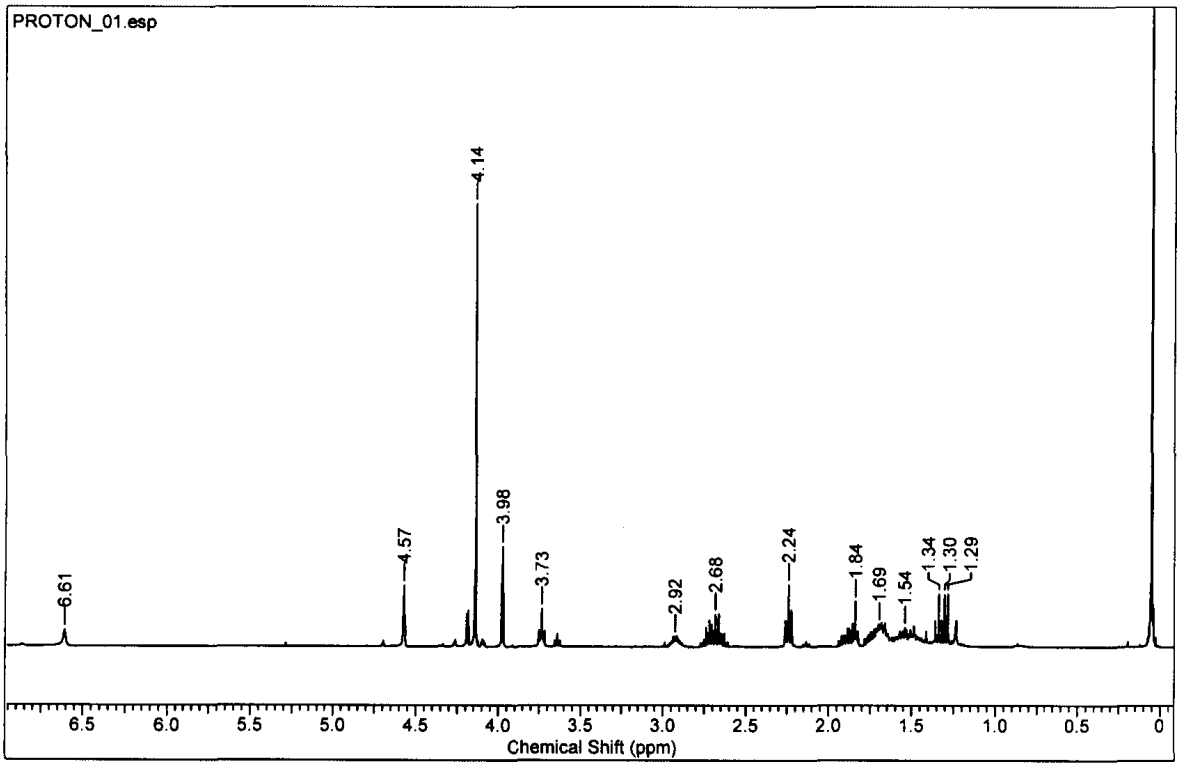

Fig. 3.2 ^{1}H NMR spectrum of **8** in $CDCl_3$.

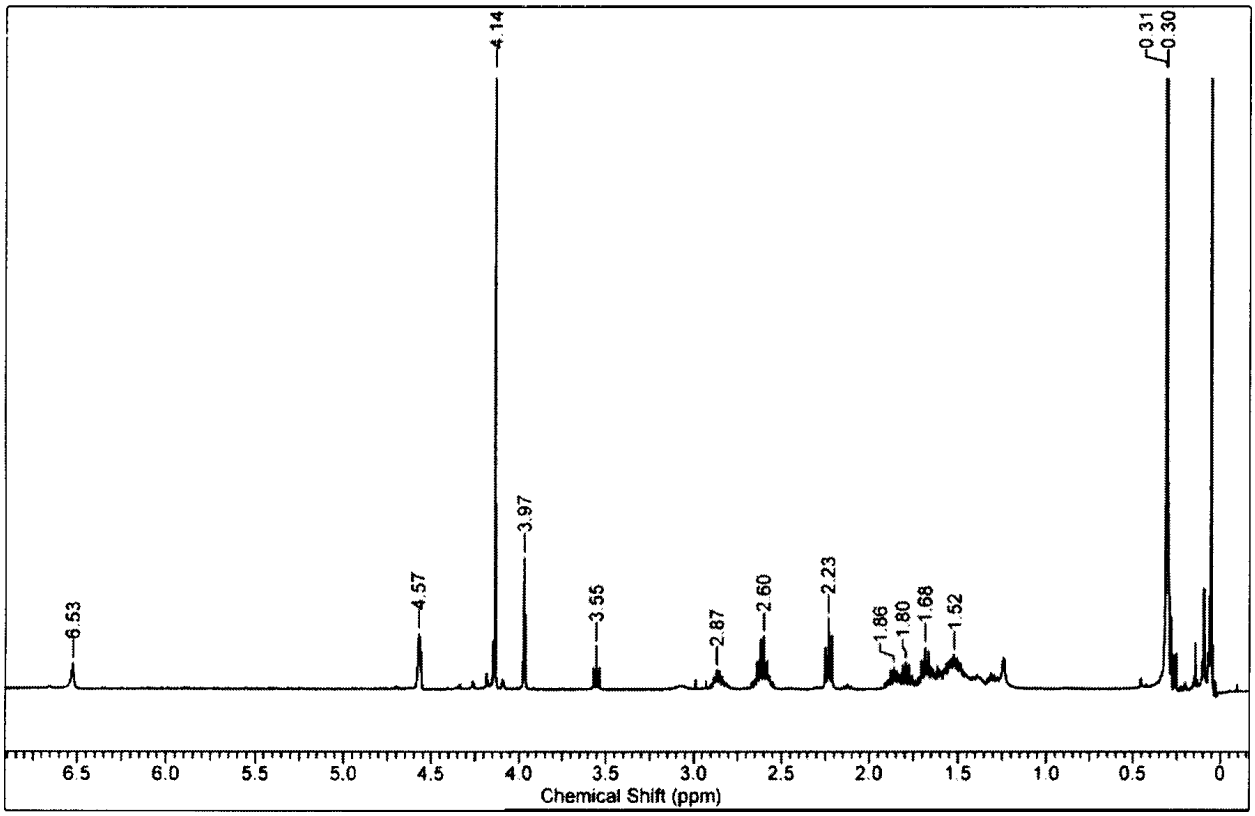

Fig. 3.3 ^{1}H NMR spectrum of **9** in $CDCl_3$.

The ^{1}H NMR spectrum of the silver-thiolate cluster **12** displays broad peaks in both the ferrocenyl and the aliphatic regions. Three peaks at 4.72, 4.14 and 3.94 ppm in the ferrocenyl region and two peaks at 1.51 and 1.00 ppm in the aliphatic region assigned to PPr_3 ligands are distinguishable in the spectrum. Via integration (considering 9 hydrogen atoms in the ferrocenyl region and 13 hydrogen atoms in the aliphatic region for the ferrocene based ligand used **9**), the integration of the peaks in the ^{1}H NMR spectrum of **12** suggest a ratio of 2:1 for ferrocenyl : tri-n-propylphosphine in the final product.

This is consistent with energy-dispersive X-ray spectroscopy (EDX) measurements for samples of **12**. According to EDX measurements the ratio of Ag:S:Fe:P is 4:4:2:1.

Thus a general formula of $[Ag_4(C_{18}H_{23}FeNOS_2)_2(PC_9H_{21})]_n$ can be proposed for **12** using the NMR and EDX analysis data. Elemental analysis of **12** also partially supports this formulation (calculated: C 39.43, H 4.93, N 2.04, S 9.34 %; found C 37.18, H 4.97, N 1.85, S 9.65 %).

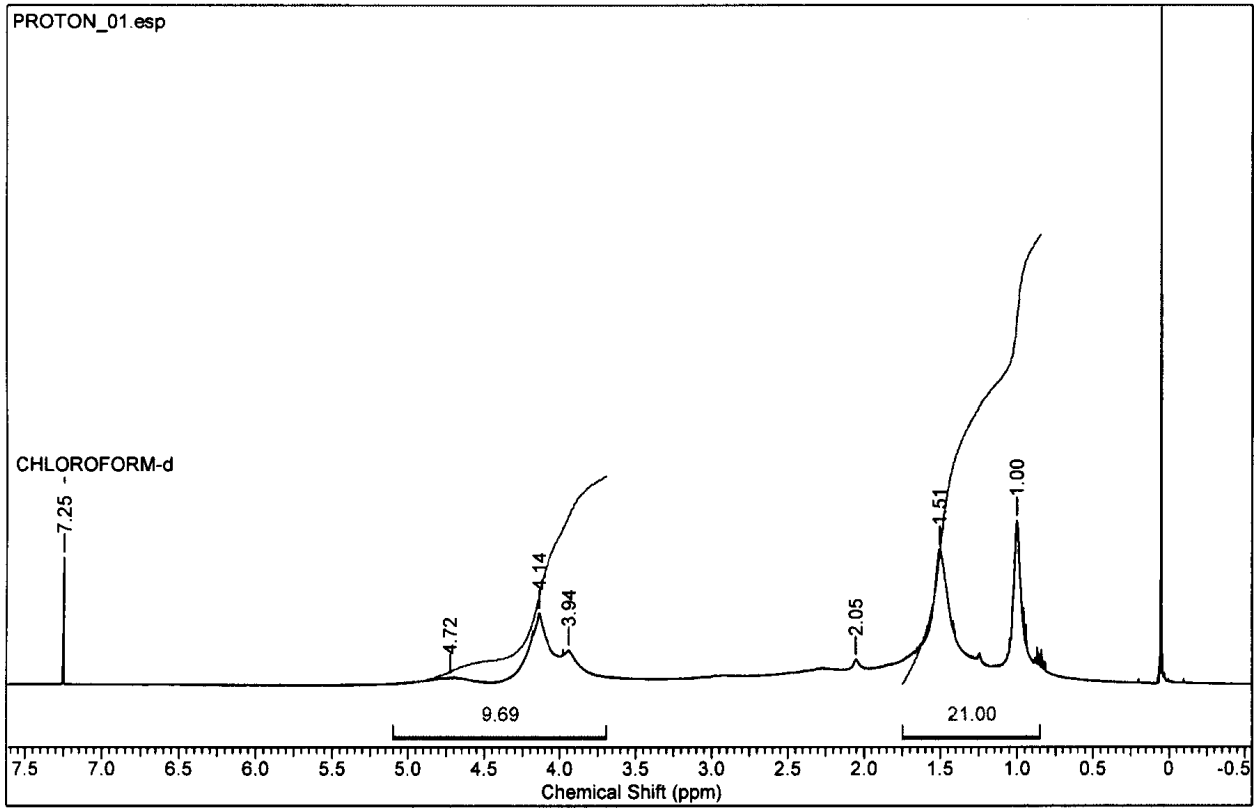

Fig. 3.4 ^1H NMR spectrum of **12** in $CDCl_3$.

3.3.2.2 UV-Vis Absorption Spectroscopy

The absorption spectra of complexes **6** and **7** are presented in Fig. 3.5. **6** shows a shoulder at ~445 nm assigned to the Fe(II) d-d transitions with ε~800 $M^{-1}cm^{-1}$, which is overlapping with a stronger absorption at higher energy. The absorption at higher energy did not resolve even at very low concentrations. In the absorption spectrum of **7**, no resolved peak was observed. This spectrum shows a very intense broad absorption with an onset at ~ 500 nm.

Fig. 3.6 presents the absorption spectrum of **12** in CH_2Cl_2 for two different concentrations. The spectrum of the concentrated solution shows a maximum at 470 nm, which is again assigned to d-d transitions in ferrocene and is slightly red shifted compared to the related maximum in the absorption spectrum of **2**. This maximum is also overlapping with absorptions at higher energies, with one shoulder at 280 nm resolved at lower concentration.

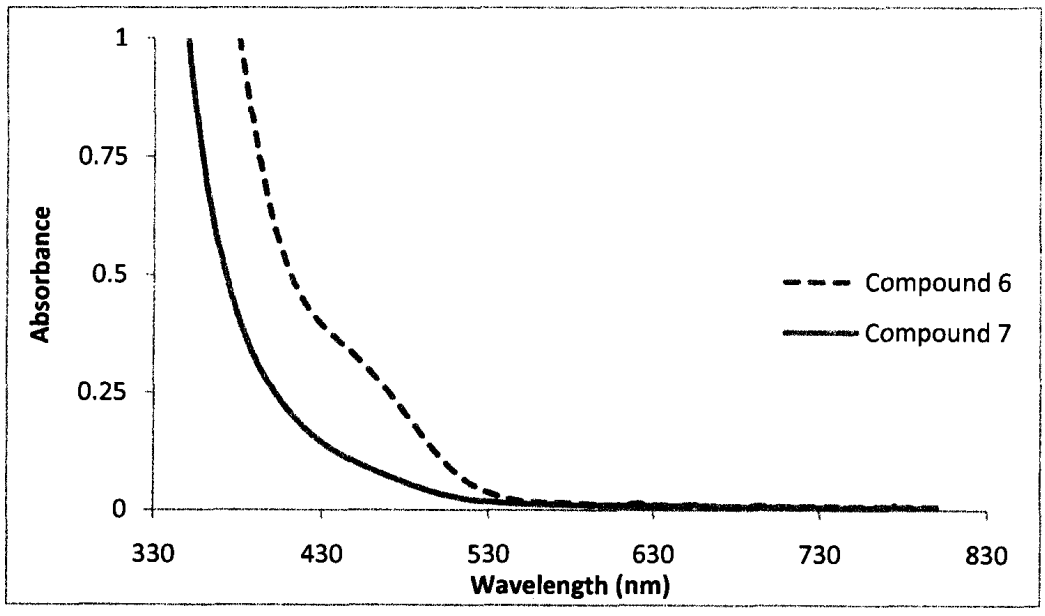

Fig. 3.5 Absorption spectra of **6** and **7** in CH_2Cl_2

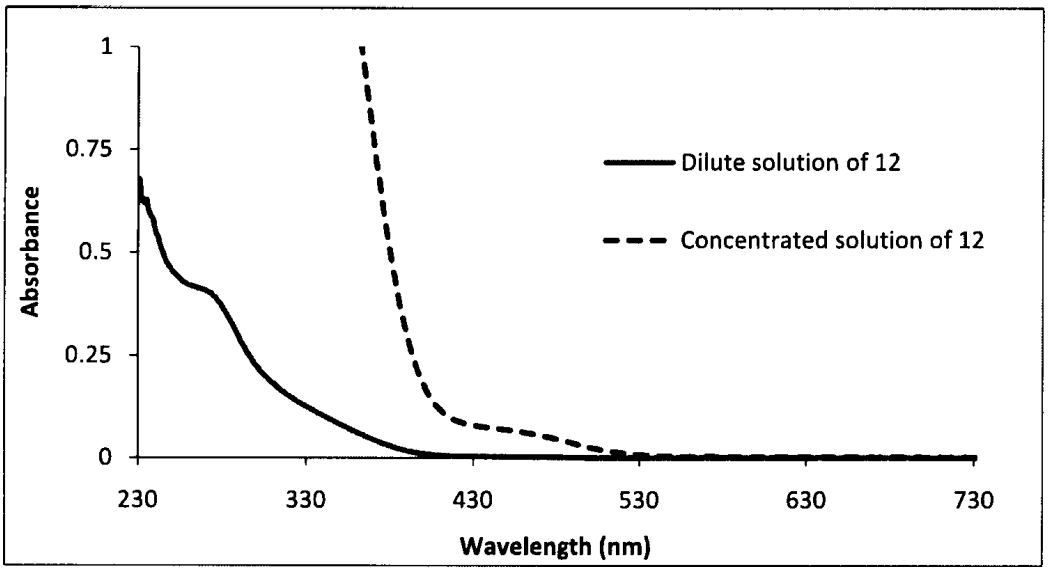

Fig. 3.6 Absorption spectra of **12** in CH_2Cl_2

3.3.2.3 Cyclic Voltammetry

Cyclic voltammetric measurements on dilute solutions of **6** (0.5 mM) and **12** (1 g L^{-1}) were performed using a 3-electrode system, with glassy carbon working electrode, platinum flag counter electrode, and a silver wire reference electrode in CH_2Cl_2 with $[NBu_4][PF_6]$ (0.1 M) as the supporting electrolyte. The potentials are reported versus S.C.E. and were referenced internally to ferrocene (475 mV),[11] added at the end of the experiments. A typical voltammogram of **6** is presented in Fig. 3.7 and displays two oxidation peaks. The first peak is a reversible oxidation at $E_{1/2}$ of 400 mV which is assigned to the oxidation of Fe(II) to Fe(III) in the ferrocenyl moiety. The ΔE ($|E_{pa}-E_{pc}|$) for this peak is 60 mV at a scan rate of 100 mVs^{-1}, which agrees well with the ideal ΔE for a one-electron oxidation process and the positions of peak voltage do not alter as a function of voltage scan rate. The ratio of the peak currents for this oxidation is i_{pa}/i_{pc} = 1.5, which is close to the ideal amount of 1 for reversible oxidation peaks. The second

peak is an oxidation at $E_{1/2}$ = 1205 mV, which displays a very small current compared to the one observed at lower potential. It also exhibits a very small ΔE (15 mV) and i_{pa}/i_{pc} ~ 3 at this scan rate. Although the potential for this second wave is close to that observed for the disulfide linkage in **2**, these voltammetry measurements were performed on solutions of single crystals of **6**, the purity for which was confirmed by ^{1}H NMR spectroscopy and elemental analysis. Furthermore, ^{1}H NMR spectra of **6** in the presence of $[NBu_4][PF_6]$ did not show any peaks corresponding to the reformation of the dithiolane ligand (**2**) (i.e. via reductive elimination). The nature of this additional redox peak is unknown but may be caused by partial detachment of the ligand upon oxidation of the Fe(II) centres.

Fig. 3.8 displays a typical voltammogram of **12**, which presents two oxidation waves. The first oxidation at $E_{1/2}$ of 380 mV can be assigned to the oxidation of Fe(II) to Fe(III) in the ferrocenyl moiety. For this peak $\Delta E = |E_{pa}-E_{pc}|$ = 15 mV at a scan rate of 100 mVs^{-1}, which is shifted from expected value of 59 mV for a reversible single electron wave. The low value of ΔE indicates that some adsorption occurs on the surface of the electrode.[17] The ratio of anodic to cathodic currents is i_{pa}/i_{pc} = 1.1, which is very close to the ideal value of 1. The voltammogram shows a second peak at $E_{1/2}$ = 1190 mV with ΔE = 5 mV and the current for the return peak is close to zero that indicates this oxidation is not a reversible oxidation. Again, detachment of the sulfur atoms from the cluster core may be the reason for the presence of this peak.

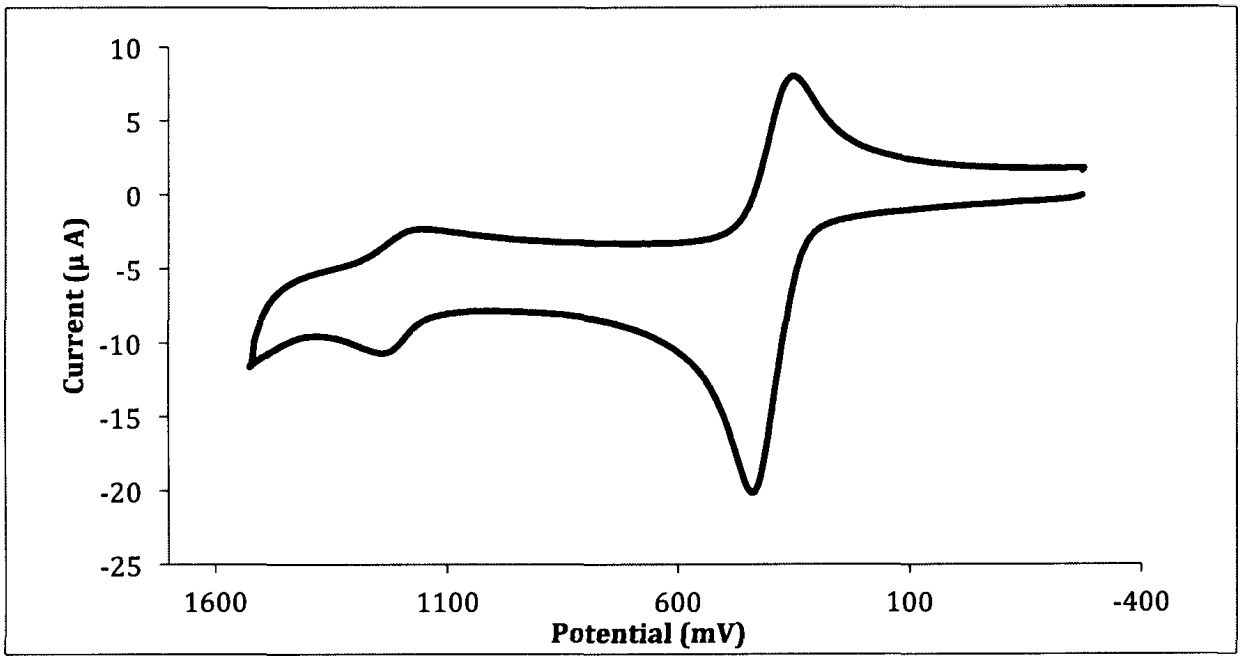

Fig. 3.7 Cyclic voltammogram of **6** in CH_2Cl_2 with $[NBu_4][PF_6]$ (0.1 M) as the supporting electrolyte and a glassy carbon electrode as working electrode at a scan rate of 100 mVs^{-1}

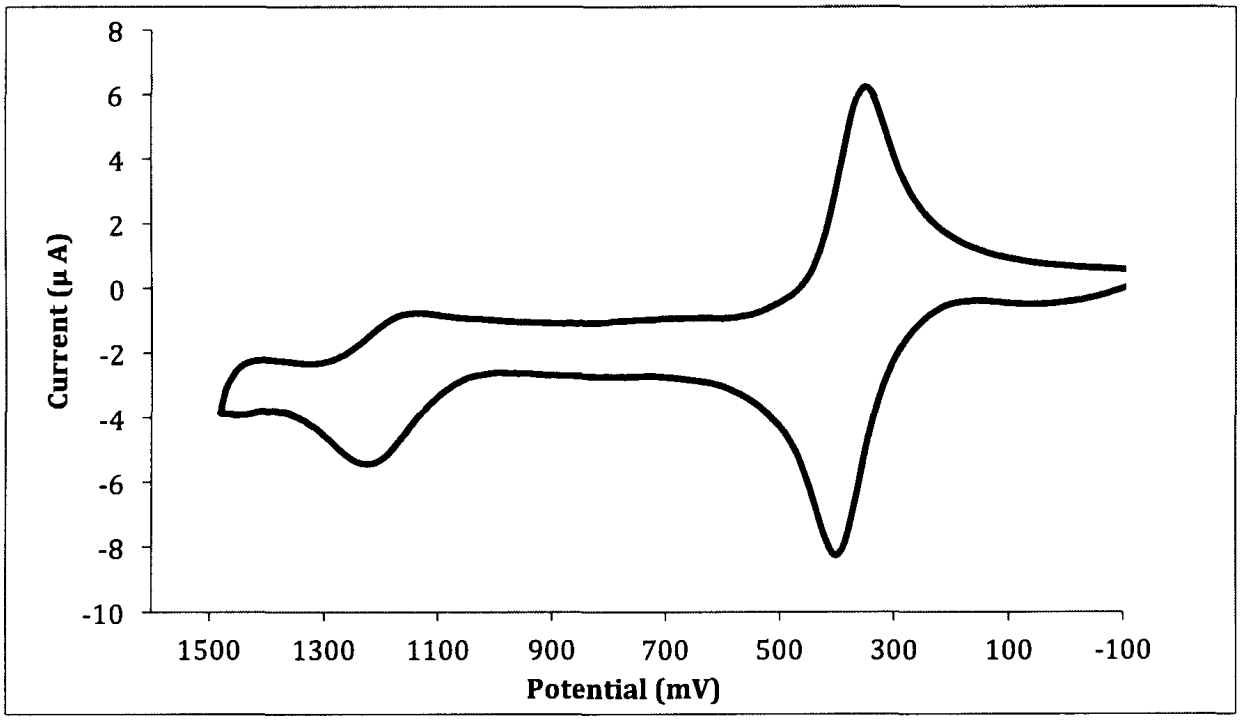

Fig. 3.8 Cyclic voltammogram of **12** in CH_2Cl_2 with $[NBu_4][PF_6]$ (0.1 M) as the supporting electrolyte and a glassy carbon electrode as working electrode at a scan rate of 100 mVs^{-1}

3.3.2.4 X-ray Crystallography

Dark orange crystals of **6** were obtained by recrystallization from $CHCl_3$/pentane and the structure determined using single crystal X-ray diffraction techniques. The ligated complex **6** crystallizes in the triclinic space group P $\bar{1}$. The molecular structure of one of the two independent molecules present in the asymmetric unit is shown in Fig. 3.9. The coordination geometry of platinum center is a slightly distorted square planar with two phosphines and one dithiolate ligand that coordinates in a bidentate fashion to yield a six-membered ring. Pt-S bond lengths (2.3352(5)-2.3603(4) Å), Pt-P bond lengths (2.2871(4)-2.3056(4)), S-Pt-S (average of 91.72°) and P-Pt-P angles (average of 97.06°) compare well with those reported for the related complexes.[6] The Cp rings defined by C11-C51 and C61-C101 are almost perfectly parallel. Selected bond lengths and angles are summarized in Table 3.1.

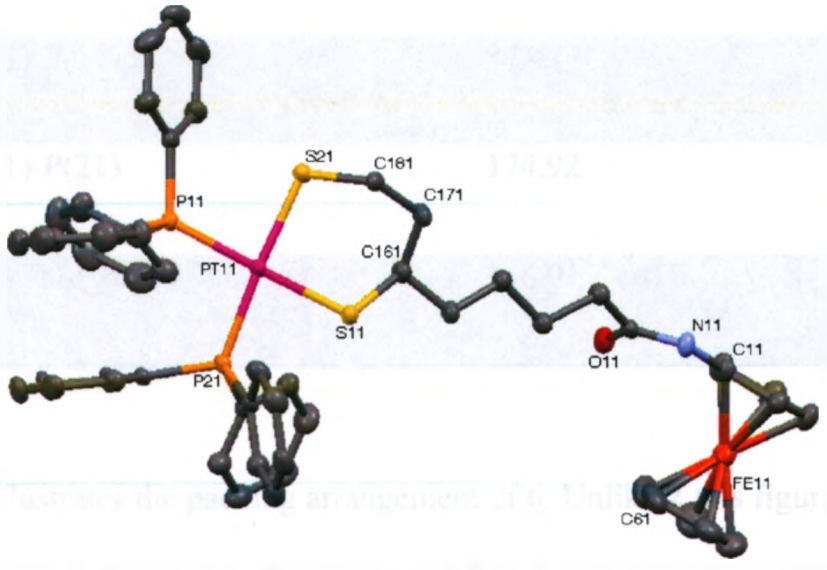

Fig. 3.9 Molecular structure of **6**

Table 3.1 Selected bond lengths [Å] and angles [°] for **6** (molecule 1)

Pt(11)-S(11)	2.3603(4)
Pt(11)-S(21)	2.3394(4)
Pt(11)-P(11)	2.2871(4)
Pt(11)-P(21)	2.3056(4)
Fe(11)-C(11)	2.0540(3)
S(11)-C(161)	1.8412(4)
S(11)-Pt(11)-S(21)	91.73
S(11)-Pt(11)-P(11)	179.10
P(11)-Pt(11)-P(21)	97.50
S(21)-Pt(11)-P(11)	87.41
S(21)-Pt(11)-P(21)	174.92
C(161)-C(171)-C(181)	116.01

Fig. 3.10 illustrates the packing arrangement of **6**. Unlike **2** this figure shows that there is no significant H-bonding in the packing of **6** and can perhaps be attributed to the large number of $CHCl_3$ present.

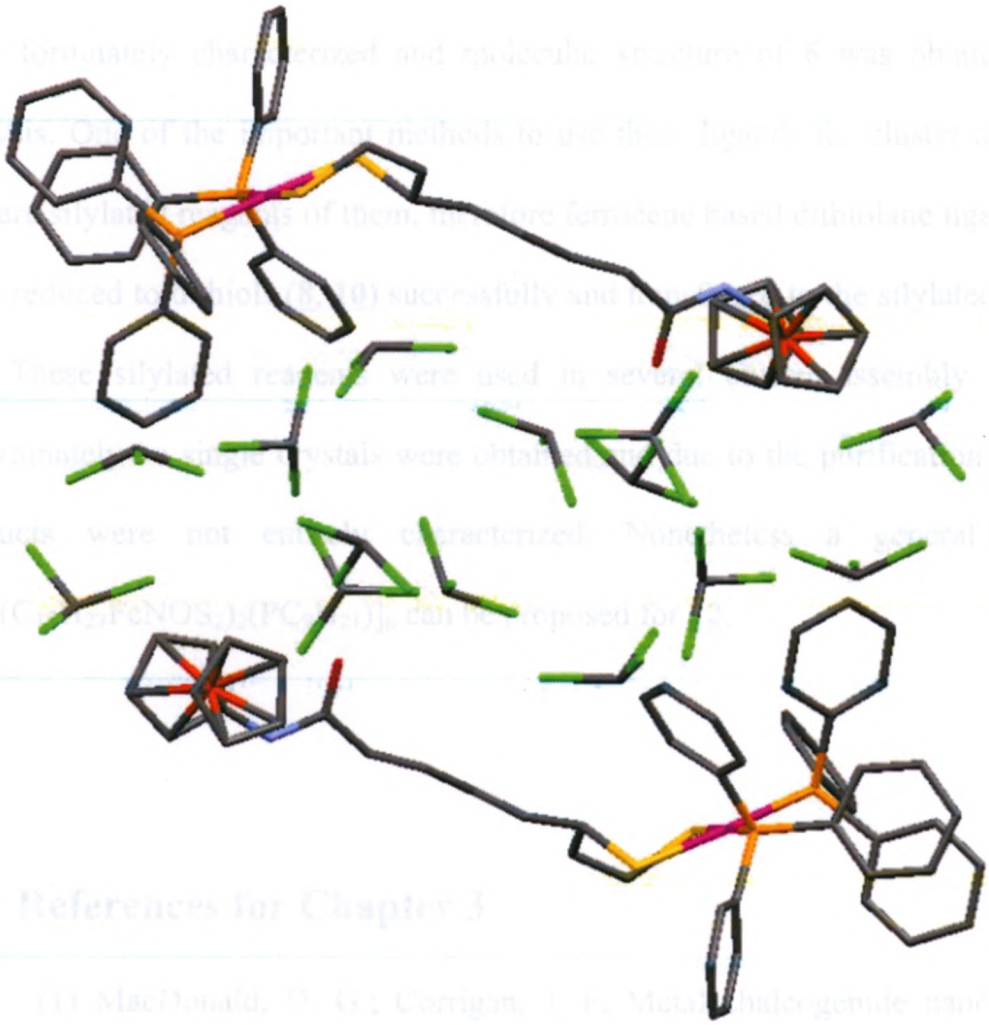

Fig. 3.10 The packing arrangement of **6**. Hydrogen atoms have been omitted for clarity.

3.4 Conclusion

To verify the reactivity of the synthesized ferrocene based dithiolane ligands their complexation were studied using oxidative addition of their S-S bonds to the platinum center. Although the purification of these complexes was challenging, they were fortunately characterized and molecular structure of **6** was obtained by X-ray analysis. One of the important methods to use these ligands for cluster assembly is to prepare silylated reagents of them, therefore ferrocene based dithiolane ligands (**2** and **3**) were reduced to dithiols (**8**, **10**) successfully and transferred to the silylated reagents (**9**, **11**). These silylated reagents were used in several cluster assembly reactions but unfortunately no single crystals were obtained and due to the purification problems the products were not entirely characterized. Nonetheless a general formula of $[Ag_4(C_{18}H_{23}FeNOS_2)_2(PC_9H_{21})]_n$ can be proposed for **12**.

3.5 References for Chapter 3

(1) MacDonald, D. G.; Corrigan, J. F. Metal chalcogenide nanoclusters with 'tailored' surfaces via 'designer' silylated chalcogen reagents. *Phil. Trans. R. Soc. A* **2010**, *368*, 1455-1472.

(2) Wallbank, A. I.; Corrigan, J. F. 1,1 '-Bis(trimethylsilylseleno)ferrocene in cluster synthesis: a redox active surface on a copper-selenide core. *Chem. Commun.* **2001**, 377-378.

(3) Lebold, T. P.; Stringle, D. L. B.; Workentin, M. S.; Corrigan, J. F. Functionalizing the surface of II-VI clusters: redox active centres on the adamantoid complex $[Cd_4Cl_4\{\mu\text{-}(SeC_5H_4)Fe(C_5H_5)\}_6]^{2-}$ *Chem. Commun.* **2003**, 1398-1399.

(4) Bonnington, K. J.; Jennings, M. C.; Puddephatt, R. J. Oxidative Addition of S-S Bonds to Dimethylplatinum(II) Complexes: Evidence for a Binuclear Mechanism. *Organometallics* **2008**, *27*, 6521-6530.

(5) Jacob, T.; Blanco, M.; Goddard, W. A. Linking molecular switches to platinum electrodes studied with DFT. *J. Phys. Chem. C* **2007**, *111*, 2749-2758.

(6) Siemeling, U.; Bretthauer, F.; Bruhn, C. Oxidative addition of asparagusic acid based disulfides to Pt(0). *J. Organomet. Chem.* **2010**, *695*, 626-629.

(7) Ohsaku, M.; Allinger, N. L. Molecular-Structure and Conformational Stability of Ethyl Methyl Disulfide - a Model of Cystine. *J. Phys. Chem.* **1988**, *92*, 4591-4594.

(8) Boyd, R. J.; Perkyns, J. S.; Ramani, R. Conformations of Simple Disulfides and L-Cystine. *Canadian Journal of Chemistry-Revue Canadienne de Chimie* **1983**, *61*, 1082-1085.

(9) Higashi, L. S.; Lundeen, M.; Seff, K. Empirical Relations between Disulfide Bond Lengths, (N Or C)-C-S-S Torsion Angles, and Substituents in Aromatic Disulfides - Crystal and Molecular-Structure of 3,3'-Dihydroxydi-2-Pyridyl Disulfide. *J. Am. Chem. Soc.* **1978**, *100*, 8101-8106.

(10) Yoshida, T.; Matsuda, T.; Otsuka, S. Tetrakis(triethylphosphine)platinum(0) *Inorganic Syntheses* **1990**, *28*, 122-123.

(11) Aranzaes, J. R.; Daniel, M. C.; Astruc, D. Metallocenes as references for the determination of redox potentials by cyclic voltammetry - Permethylated iron and cobalt sandwich complexes, inhibition by polyamine dendrimers, and the role of hydroxy-containing ferrocenes. *Can. J. Chem.* **2006**, *84*, 288-299.

(12) Davison, A.; Edelstein, N.; Holm, R. H.; Maki, A. H. Further Examples of Complexes Related by Electron-Transfer Reactions - Complexes Derived from Bis(trifluoromethyl)-1,2-Dithietene. *Inorg. Chem.* **1964**, *3*, 814-817.

(13) Weigand, W.; Bosl, G.; Vondielingen, B.; Gollnick, K. Metal-Complexes of Functionalized Sulfur-Containing Ligands .8. 4-Phenyl-1,2-Dithiolane-1-Oxide, a Stable, 5-Membered Cyclic Thiosulfinate. *B: Chem. Sci.* **1994**, *49*, 513-518.

(14) Siemeling, U.; Bretthauer, F.; Bruhn, C.; Fellinger, T.; Tong, W.; Chan, M. C. W. Gold Nanoparticles Bearing an alpha-Lipoic Acid-based Ligand Shell. Synthesis, Model Complexes and Studies Concerning Phosphorescent Platinum(II)-Functionalisation. *B: Chem. Sci.* **2010**, *65*, 1089-1096.

(15) Power, W. P.; Wasylishen, R. E. Anisotropies of the P-31 Chemical-Shift and P-31-Pt-195 Indirect Spin Spin Coupling in Platinum(II) Phosphines. *Inorg. Chem.* **1992**, *31*, 2176-2183.

(16) Weigand, W.; Wunsch, R.; Polborn, K. Metal complexes of functionalized sulfur-containing ligands, part 13. Oxidative addition of 2,3,4-benzotrithiepin 1-oxide to

platinum(0) compounds: a convenient synthetic route to platinum(II) thiosulfinato complexes. *Inorg. Chim. Acta* **1998**, *273*, 106-110.

(17) Labande, A.; Ruiz, J.; Astruc, D. Supramolecular gold nanoparticles for the redox recognition of oxoanions: Syntheses, titrations, stereoelectronic effects, and selectivity. *J. Am. Chem. Soc.* **2002**, *124*, 1782-1789.

4 General Conclusions and Prospective Work

4.1 Summary

The unique and interesting optical and electronic properties of metal chalcogenide clusters have aroused the interest in this field of nanoscience. The advent of trimethylsilychalcogen reagents has introduced a powerful method to synthesize metal chalcogenide nanoclusters.[1] Recently, ferrocene based ligands have been successfully incorporated onto the surface of metal chalcogenide clusters using $CpFe(C_5H_4SeSiMe_3)$ and $Fe(C_5H_4SeSiMe_3)_2$ reagents. Oxidative cleavage of the ferrocenylselenolate groups from the cluster surface, and cluster degradation have been reported for the formed clusters.[2, 3] It has been shown that the presence of a spacer between the cluster core and ferrocenyl moieties is effective in avoiding the oxidative degradation.[4, 5] Our group has reported successful usage of ferrocenyl based ligands, which contains an alkyl chain spacer to limit communication between the ferrocene and chalcogen units, in the preparation of metal-chalcogen nanoclusters.[6, 7]

The preparation and characterization of four new ferrocene based dithiolane compounds are reported in the second chapter of this thesis. Dithiolane ligands were targeted due to the fact that they have two points of attachment to the cluster core, and thus, may show an increase in the stability of the corresponding nanoclusters in solution compared to monodentate counterparts. The targeted ligands were designed to contain an amide, ester or carbonyl functional group in their structure. The presence of these functionalities may make the ligands effective for oxo-anion recognition. The synthesis and purification of these materials was a challenging one because of the sensitivity of

the S-S bond in these compounds and the formation of insoluble polymers when compounds are exposed to light or heat. Even by completing the reactions in the subdued light, the acylation of ferrocene to yield **4** and the synthesis of 2-(1, 2-dithiolan-3-yl)acetic acid, the precursor for compound **5**, had such low yields such that their preparation was not practical for the subsequent steps. Instead, compounds **2** and **3** were synthesized in high yields and were used in subsequent reactions. The cyclic voltammograms of the prepared compounds display a reversible oxidation assigned to the ferrocenyl unit and one quasi-reversible oxidation related to the dithiolane ring.

Before utilizing synthesized compounds in cluster assembly reactions, their complexation was studied using oxidative addition of their S-S bonds to the platinum center. These reactions resulted in *cis* mononuclear platinum(II) complexes. Although the purification of these complexes was difficult, they were fortunately characterized, and furthermore, the molecular structure of **6** was obtained by X-ray analysis. To prepare silylated reagents, ferrocene based dithiolane ligands (**2** and **3**) were reduced to dithiols (**8**, **10**) successfully and transferred to the silylated reagents (**9**, **11**). These silylated reagents were used in several cluster assembly reactions; however, no single crystals were obtained and due to the purification problems, the products were not entirely characterized. Nonetheless, a general formula of $[Ag_4(C_{18}H_{23}FeNOS_2)_2(PC_9H_{21})]_n$ can be proposed for **12**.

The work accomplished in this thesis has extended our knowledge about ferrocene dithiolate complexes and their functionalization onto the surface of clusters and nanoparticles. While it was anticipated that reagents containing two chalcogen atoms present the opportunity for greater coordination to the cluster surface, it was

found that working with these compounds is more difficult than initially expected due to the sensitivity of the S-S bond in dithiolane ring. The presence of long alkyl spacer between the ferrocenyl unit and the chalcogen centers is found to have negative effect on the crystallization process. It should be noted that compounds 3 and 7 were obtained as oily materials and the crystallization of **2** and **6** required a lot of effort.

More studies on the preparation and characterization of polynuclear metal chalcogenide clusters, functionalized with the synthesized ligands, are required. In this respect, different reaction conditions such as using different metals and solubilizing phosphine ligands can be investigated.

4.2 References for Chapter 4

(1) MacDonald, D. G.; Corrigan, J. F. Metal chalcogenide nanoclusters with 'tailored' surfaces via 'designer' silylated chalcogen reagents. *Phil. Trans. R. Soc. A* **2010**, *368*, 1455-1472.

(2) Lebold, T. P.; Stringle, D. L. B.; Workentin, M. S.; Corrigan, J. F. Functionalizing the surface of II-VI clusters: redox active centres on the adamantoid complex $[Cd_4Cl_4\{\mu\text{-}(SeC_5H_4)Fe(C_5H_5)\}_6]^{2-}$ *Chem. Commun.* **2003**, 1398-1399.

(3) Wallbank, A. I.; Corrigan, J. F. 1,1 '-Bis(trimethylsilylseleno)ferrocene in cluster synthesis: a redox active surface on a copper-selenide core. *Chem. Commun.* **2001**, 377-378.

(4) Astruc, D.; Daniel, M. C.; Ruiz, J. Dendrimers and gold nanoparticles as exo-receptors sensing biologically important anions. *Chem. Commun.* **2004**, 2637-2649.

(5) Labande, A.; Ruiz, J.; Astruc, D. Supramolecular gold nanoparticles for the redox recognition of oxoanions: Syntheses, titrations, stereoelectronic effects, and selectivity. *J. Am. Chem. Soc.* **2002**, *124*, 1782-1789.

(6) MacDonald, D. G., Ph.D. Thesis, University of Western Ontario, 2010.

(7) Ahmar, S.; MacDonald, D. G.; Vijayaratnam, N.; Battista, T. L.; Workentin, M. S.; Corrigan, J. F. A Nanoscopic 3D Polyferrocenyl Assembly: The Triacontakaihexa(ferrocenylmethylthiolate) $[Ag_{48}(\mu_4\text{-}S)_6(\mu_{2/3}\text{-}SCH_2Fc)_{36}]$. *Angew. Chem. Int. Ed.* **2010**, *49*, 4422-4424.

APPENDIX 1.

Crystal data and structure refinement for $C_{18}H_{23}FeNOS_2$ (**2**).

Empirical formula	$C_{18}H_{23}FeNOS_2$	
Formula weight	389.34	
Temperature	150(2) K	
Wavelength	0.71073 Å	
Crystal system	Orthorhombic	
Space group	Pca2(1)	
Unit cell dimensions	a = 10.0366(10) Å	α= 90°.
	b = 11.1816(11) Å	β= 90°.
	c = 31.259(3) Å	γ = 90°.
Volume	3508.1(6) $Å^3$	
Z	8	
Density (calculated)	1.474 Mg/m^3	
Absorption coefficient	1.101 mm^{-1}	
F(000)	1632	
Crystal size	0.09 x 0.08 x 0.03 mm^3	
Theta range for data collection	1.82 to 28.72°.	
Index ranges	-13<=h<=13, -15<=k<=15, -42<=l<=42	
Reflections collected	80156	
Independent reflections	9059 [R(int) = 0.0548]	
Completeness to theta = 28.72∞	99.9 %	
Absorption correction	None	
Max. and min. transmission	0.9730 and 0.9084	
Refinement method	Full-matrix least-squares on F^2	
Data / restraints / parameters	9059 / 29 / 409	
Goodness-of-fit on F^2	1.085	
Final R indices [I>2sigma(I)]	R1 = 0.0671, wR2 = 0.1697	
R indices (all data)	R1 = 0.0828, wR2 = 0.1789	
Absolute structure parameter	0.14(3)	
Largest diff. peak and hole	1.226 and -1.132 e. $Å^{-3}$	

Atomic coordinates (x 10^4) and equivalent isotropic displacement parameters ($Å^2$x 10^3) for **2**. U(eq) is defined as one third of the trace of the orthogonalized U^{ij} tensor.

	x	y	z	U(eq)
Fe(11)	12206(1)	8343(1)	9774(1)	26(1)
S(11)	11421(2)	1824(3)	11864(1)	68(1)
S(21)	9970(3)	1238(3)	12258(1)	94(1)
N(11)	13081(4)	5696(4)	9938(2)	28(1)
O(11)	10904(4)	5205(4)	10023(2)	39(1)
C(11)	12917(5)	6676(5)	9650(2)	27(1)
C(21)	11834(6)	6919(5)	9380(2)	33(1)
C(31)	12173(5)	7943(7)	9134(2)	35(1)
C(41)	13469(6)	8333(5)	9260(2)	31(1)
C(51)	13927(5)	7544(5)	9576(2)	30(1)
C(61)	10594(6)	8610(7)	10161(3)	50(2)
C(71)	10795(6)	9592(5)	9895(2)	36(1)
C(81)	12073(6)	10053(6)	9983(2)	36(1)
C(91)	12647(6)	9341(6)	10298(2)	39(1)
C(101)	11753(8)	8416(6)	10409(2)	42(2)
C(111)	12084(5)	5073(6)	10112(2)	30(1)
C(121)	12553(7)	4158(6)	10446(2)	38(1)
C(131)	11573(7)	3160(6)	10521(2)	43(2)
C(141)	11960(9)	2377(8)	10887(2)	55(2)
C(151)	10856(12)	1490(10)	11012(3)	78(3)
C(161)	11033(10)	848(8)	11402(3)	69(2)
C(171)	9769(12)	80(10)	11497(4)	101(4)
C(181)	8911(14)	721(15)	11843(4)	57(4)
C(181)	9761(18)	-54(17)	11988(4)	59(4)
Fe(12)	11803(1)	13342(1)	13694(1)	25(1)
N(12)	12647(5)	10696(5)	13515(2)	31(1)
O(12)	10472(4)	10227(4)	13434(1)	34(1)

C(12)	12513(5)	11641(5)	13806(2)	27(1)
C(22)	13517(5)	12507(5)	13877(2)	31(1)
C(32)	13048(5)	13313(6)	14206(2)	31(1)
C(42)	11768(6)	12932(6)	14328(2)	34(1)
C(52)	11410(6)	11911(5)	14085(2)	30(1)
C(62)	11396(8)	13452(6)	13055(2)	41(2)
C(72)	12260(6)	14398(6)	13179(2)	38(1)
C(82)	11622(7)	15086(6)	13495(2)	38(1)
C(92)	10348(7)	14588(7)	13567(2)	43(2)
C(102)	10200(6)	13570(6)	13302(3)	43(2)
C(112)	11643(5)	10050(6)	13335(2)	31(1)
C(122)	12102(6)	9188(7)	13002(2)	41(1)
C(132)	11115(7)	8167(6)	12924(2)	47(2)
C(142)	11555(10)	7327(7)	12569(3)	62(2)
C(152)	10759(14)	6243(13)	12426(4)	59(3)
C(152)	10216(14)	6646(13)	12461(4)	17(2)
S(12)	10370(4)	6841(3)	11592(1)	63(1)
S(22)	10309(5)	5223(4)	11299(2)	83(1)
C(162)	9731(13)	6602(11)	12111(4)	60(3)
C(172)	8750(19)	5551(15)	11993(6)	98(6)
C(182)	9118(17)	4572(14)	11648(5)	87(5)
S(1)	11276(17)	6709(13)	11620(5)	128(4)
S(2)	10348(10)	5989(11)	11178(4)	97(3)
C(162)	10484(14)	5757(13)	12096(5)	23(3)
C(172)	9330(20)	4870(20)	11977(7)	49(5)
C(182)	9980(40)	4770(30)	11520(8)	81(9)

APPENDIX 2

Crystal data and structure refinement for *cis*-$Pt(PPh_3)_2(C_{18}H_{23}FeNOS_2)$ (**6**).

Empirical formula	$C_{57.50}\ H_{56.50}\ Cl_{10.50}\ Fe\ N\ O\ P_2\ Pt\ S_2$	
Formula weight	1526.76	
Temperature	150(2) K	
Wavelength	0.71073 Å	
Crystal system	Triclinic	
Space group	P -1	
Unit cell dimensions	a = 16.910(3) Å	α= 90.122(9)°.
	b = 20.310(4) Å	β= 103.733(6) °.
	c = 20.370(4) Å	γ = 111.205(5) °.
Volume	6306(2) $Å^3$	
Z	4	
Density (calculated)	1.608 Mg/m^3	
Absorption coefficient	3.047 mm^{-1}	
F(000)	3044	
Crystal size	0.10 x 0.06 x 0.05 mm^3	
Theta range for data collection	1.03 to 31.70°.	
Index ranges	-24<=h<=24, -29<=k<=29, -30<=l<=29	
Reflections collected	353324	
Independent reflections	42107 [R(int) = 0.1624]	
Completeness to theta = 31.70∞	98.7 %	
Absorption correction	None	
Refinement method	Full-matrix least-squares on F^2	
Data / restraints / parameters	42107 / 0 / 1369	
Goodness-of-fit on F^2	1.001	
Final R indices [I>2sigma(I)]	R1 = 0.0551, wR2 = 0.1133	
R indices (all data)	R1 = 0.1275, wR2 = 0.1449	
Largest diff. peak and hole	2.797 and -1.807 e. $Å^{-3}$	

Atomic coordinates (x 10^4) and equivalent isotropic displacement parameters ($Å^2$x 10^3) for **6**. U(eq) is defined as one third of the trace of the orthogonalized U^{ij} tensor.

	x	y	z	U(eq)
Pt(11)	1211(1)	-857(1)	-2579(1)	20(1)
Fe(11)	2782(1)	1549(1)	3512(1)	36(1)
S(11)	598(1)	-991(1)	-1637(1)	22(1)
S(21)	725(1)	61(1)	-2918(1)	27(1)
P(11)	1791(1)	-718(1)	-3499(1)	20(1)
P(21)	1607(1)	-1785(1)	-2182(1)	21(1)
O(11)	2854(3)	1814(2)	1699(2)	32(1)
N(11)	1654(3)	1686(2)	2084(2)	24(1)
C(11)	2099(4)	1963(3)	2767(3)	27(1)
C(21)	2977(4)	2457(3)	3011(3)	36(2)
C(26)	336(4)	-1848(3)	-4199(3)	34(1)
C(31)	3113(5)	2616(4)	3720(3)	44(2)
C(41)	2331(5)	2235(3)	3905(3)	38(2)
C(51)	1694(4)	1812(3)	3320(3)	30(1)
C(61)	2715(7)	604(5)	3110(5)	64(3)
C(71)	3595(7)	1095(6)	3285(5)	73(3)
C(81)	3826(6)	1294(6)	3987(5)	71(3)
C(91)	3084(6)	925(5)	4243(4)	58(2)
C(101)	2398(6)	507(4)	3698(4)	54(2)
C(111)	2049(4)	1656(3)	1589(3)	25(1)
C(121)	1459(4)	1439(3)	880(3)	28(1)
C(131)	1505(4)	790(3)	544(3)	27(1)
C(141)	1143(4)	702(3)	-224(3)	29(1)
C(151)	1036(4)	-12(3)	-556(3)	27(1)
C(161)	890(4)	-64(3)	-1315(3)	29(1)
C(171)	255(4)	260(3)	-1696(3)	30(1)
C(181)	-91(4)	47(3)	-2462(3)	24(1)
C(191)	2982(4)	-443(3)	-3320(3)	27(1)
C(201)	3418(4)	-310(3)	-3841(4)	38(2)
C(211)	4318(5)	-59(4)	-3698(4)	49(2)

C(221)	4807(5)	86(4)	-3028(4)	53(2)
C(231)	4400(4)	-10(4)	-2517(4)	47(2)
C(241)	3479(4)	-282(3)	-2656(3)	34(1)
C(251)	1245(4)	-1519(3)	-4101(3)	25(1)
C(271)	-148(5)	-2404(4)	-4695(3)	43(2)
C(281)	273(5)	-2638(3)	-5103(3)	43(2)
C(291)	1172(5)	-2328(3)	-4998(3)	39(2)
C(301)	1659(4)	-1771(3)	-4499(3)	31(1)
C(311)	1664(4)	-24(3)	-4040(3)	28(1)
C(321)	2176(5)	687(3)	-3790(3)	36(2)
C(331)	2103(6)	1232(4)	-4173(4)	50(2)
C(341)	1524(6)	1073(4)	-4802(5)	57(2)
C(351)	1030(5)	387(5)	-5066(4)	51(2)
C(361)	1092(5)	-167(4)	-4686(3)	38(2)
C(371)	659(4)	-2502(3)	-2009(3)	24(1)
C(381)	743(4)	-2969(3)	-1526(3)	30(1)
C(391)	4(4)	-3534(3)	-1449(3)	35(1)
C(401)	-810(5)	-3622(3)	-1848(3)	37(2)
C(411)	-904(4)	-3159(3)	-2334(4)	37(2)
C(421)	-173(4)	-2599(3)	-2412(3)	32(1)
C(431)	2487(4)	-1548(3)	-1397(3)	27(1)
C(441)	2758(4)	-887(3)	-1036(3)	30(1)
C(451)	3417(5)	-709(4)	-427(3)	43(2)
C(461)	3805(5)	-1179(4)	-183(4)	50(2)
C(471)	3547(4)	-1835(4)	-536(3)	40(2)
C(481)	2899(4)	-2020(3)	-1144(3)	33(1)
C(491)	1975(4)	-2268(3)	-2730(3)	24(1)
C(501)	1367(4)	-2839(3)	-3182(3)	29(1)
C(511)	1638(5)	-3181(3)	-3621(3)	40(2)
C(521)	2509(5)	-2958(3)	-3619(3)	40(2)
C(531)	3124(5)	-2387(3)	-3176(4)	40(2)
C(541)	2858(4)	-2046(3)	-2728(3)	29(1)
Pt(12)	1175(1)	-3396(1)	2442(1)	19(1)
Fe(12)	2694(1)	-4856(1)	8475(1)	34(1)

S(12)	577(1)	-3637(1)	3390(1)	22(1)
S(22)	728(1)	-4604(1)	2112(1)	27(1)
P(12)	1781(1)	-3174(1)	1534(1)	21(1)
P(22)	1546(1)	-2228(1)	2821(1)	20(1)
O(12)	2912(3)	-5162(2)	6673(2)	41(1)
N(12)	1698(3)	-5718(2)	7059(2)	28(1)
C(12)	2130(4)	-5699(3)	7746(3)	29(1)
C(22)	3018(4)	-5601(4)	8035(3)	41(2)
C(32)	3130(5)	-5658(4)	8743(4)	48(2)
C(42)	2313(5)	-5804(4)	8888(3)	43(2)
C(52)	1689(4)	-5822(3)	8285(3)	31(1)
C(62)	2485(5)	-4006(3)	8027(4)	48(2)
C(72)	3399(5)	-3899(4)	8195(4)	56(2)
C(82)	3661(5)	-3919(4)	8917(4)	54(2)
C(92)	2921(5)	-4041(4)	9181(4)	45(2)
C(102)	2195(5)	-4103(3)	8636(4)	44(2)
C(112)	2106(4)	-5462(3)	6563(3)	29(1)
C(122)	1523(4)	-5565(3)	5861(3)	31(1)
C(132)	1551(4)	-4880(3)	5552(3)	29(1)
C(142)	1180(4)	-4994(3)	4789(3)	29(1)
C(152)	1043(4)	-4353(3)	4474(3)	30(1)
C(162)	901(4)	-4377(3)	3708(3)	29(1)
C(172)	265(4)	-5095(3)	3330(3)	30(1)
C(182)	-78(4)	-5081(3)	2575(3)	26(1)
C(192)	2967(4)	-2681(3)	1778(3)	29(1)
C(202)	3468(4)	-2447(3)	1313(4)	38(2)
C(212)	4375(5)	-2058(4)	1546(5)	51(2)
C(222)	4775(5)	-1925(4)	2229(5)	59(2)
C(232)	4294(5)	-2180(4)	2690(4)	50(2)
C(242)	3392(4)	-2561(3)	2469(3)	33(1)
C(252)	1716(4)	-3942(3)	1021(3)	31(1)
C(262)	2259(5)	-4309(3)	1294(3)	35(2)
C(272)	2208(5)	-4913(4)	947(4)	47(2)
C(282)	1612(6)	-5155(4)	314(4)	54(2)

C(292)	1105(5)	-4788(4)	31(4)	50(2)
C(302)	1141(4)	-4183(3)	372(3)	36(1)
C(312)	1223(4)	-2740(3)	905(3)	22(1)
C(322)	313(4)	-2970(3)	801(3)	32(1)
C(332)	-189(5)	-2744(4)	286(3)	41(2)
C(342)	212(5)	-2272(4)	-139(3)	40(2)
C(352)	1106(5)	-2025(3)	-27(3)	39(2)
C(362)	1619(4)	-2252(3)	486(3)	32(1)
C(372)	2458(4)	-1890(3)	3592(3)	25(1)
C(382)	2740(4)	-2360(3)	3979(3)	30(1)
C(392)	3428(4)	-2112(4)	4572(3)	38(2)
C(402)	3819(5)	-1395(4)	4777(3)	44(2)
C(412)	3540(4)	-919(4)	4383(3)	39(2)
C(422)	2868(4)	-1166(3)	3793(3)	34(1)
C(432)	1861(4)	-1543(3)	2244(3)	22(1)
C(442)	2724(4)	-1226(3)	2206(3)	28(1)
C(452)	2940(4)	-750(3)	1725(3)	34(1)
C(462)	2293(4)	-584(3)	1277(3)	33(1)
C(472)	1433(4)	-895(3)	1318(3)	33(1)
C(482)	1214(4)	-1372(3)	1796(3)	27(1)
C(492)	614(4)	-2090(3)	3026(3)	24(1)
C(502)	708(4)	-1570(3)	3523(3)	29(1)
C(512)	-37(5)	-1475(4)	3618(3)	37(2)
C(522)	-852(4)	-1889(3)	3231(3)	36(2)
C(532)	-962(4)	-2409(3)	2748(3)	35(1)
C(542)	-225(4)	-2509(3)	2641(3)	29(1)
Cl(11)	4796(2)	-3840(1)	11828(1)	80(1)
Cl(21)	5137(2)	-3103(1)	10648(1)	81(1)
Cl(31)	4353(2)	-4631(1)	10529(1)	76(1)
Cl(12)	5679(2)	-3397(2)	3579(2)	116(1)
Cl(22)	6459(3)	-3893(2)	4778(1)	134(2)
Cl(32)	7513(2)	-3108(1)	3919(2)	96(1)
Cl(13)	3976(2)	-3928(2)	5275(1)	99(1)
Cl(23)	4648(2)	-3185(1)	6613(2)	86(1)

Cl(33)	5091(2)	-4370(1)	6339(1)	69(1)
Cl(14)	3297(2)	-4037(1)	3484(1)	70(1)
Cl(24)	2558(2)	-5490(1)	3784(1)	69(1)
Cl(34)	3261(2)	-5194(2)	2627(1)	69(1)
Cl(15)	5383(2)	-880(2)	8608(2)	132(2)
Cl(25)	6135(2)	-1427(2)	9759(1)	101(1)
Cl(35)	4979(2)	-2370(1)	8602(2)	90(1)
Cl(16)	6765(1)	-1097(1)	1541(1)	56(1)
Cl(26)	7552(1)	-2077(1)	1243(1)	58(1)
Cl(36)	6838(1)	-2211(1)	2411(1)	49(1)
Cl(17)	3500(2)	-6610(2)	10323(1)	88(1)
Cl(27)	4331(2)	-6020(1)	11711(1)	75(1)
Cl(37)	2444(1)	-6641(1)	11251(1)	65(1)
C(1S)	4465(6)	-3846(4)	10964(4)	62(2)
C(2S)	6481(6)	-3713(4)	3958(4)	58(2)
C(3S)	4272(5)	-4008(4)	6143(4)	50(2)
C(4S)	2714(5)	-4928(4)	3142(4)	46(2)
C(5S)	5783(5)	-1533(4)	8863(4)	45(2)
C(6S)	7379(4)	-1615(4)	1891(4)	42(2)
C(7S)	3441(5)	-6680(4)	11161(4)	45(2)